Mass spectrum of heavy Higgs bosons in two-Higgs-doublet model in the light of the CDF *W*-mass anomaly

Dong-Won Jung[1,2,*], Yongtae Heo[1,3,†] and Jae Sik Lee[1,3,‡]

[1]*Department of Physics, Chonnam National University, Gwangju 61186, Korea*
[2]*Department of Physics, Yonsei University, Seoul 03722, Korea*
[3]*IUEP, Chonnam National University, Gwangju 61186, Korea*

We analyze the mass spectrum of the charged and neutral Higgs bosons in the framework of the two Higgs doublet model (2HDM) in the light of the precision measurement of the W boson mass by the CDF collaboration. We have considered the most general 2HDM potential with explicit CP violation in the Higgs basis which contains the three CP-mixed neutral mass eigenstates H_1, H_2, and H_3 with $M_{H_1} \leq M_{H_2} \leq M_{H_3}$. The high-precision CDF measurement of the W boson mass is characterized by the large positive value of the T parameter. By identifying the lightest neutral Higgs boson H_1 as the SM-like one discovered at the LHC, we find that it is necessary to have the mass splitting between the charged Higgs boson $H^\pm$ and the second heaviest neutral one H_2 to accommodate the sizable positive deviation of the T parameter from its SM value of 0. By combining the mass splitting between $H^\pm$ and H_2 with the theoretical constraints from the perturbative unitarity and for the Higgs potential to be bounded from below, we implement comprehensive analysis of the mass spectrum of the heavy Higgs bosons taking account of the effects of deviation from the alignment limit and also the mass splitting between H_3 and H_2. We further analyze the behavior of the heavy-Higgs mass spectrum according to the variation of the T parameter. Finally, concentrating on the heavy mass region $M \equiv (M_{H_2} + M_{H^\pm})/2 \gtrsim 500$ GeV in which we find a mass hierarchy of $M \gg M_{H_1} \sim |\Delta| \gtrsim \delta$ with $\Delta \equiv M_{H_2} - M_{H^\pm}$ and $\delta \equiv M_{H_3} - M_{H_2}$, we discuss some benchmarking scenarios for the searches of heavy Higgs bosons at future colliders such as the high luminosity option of the LHC and a 100 TeV hadron collider.

I. INTRODUCTION

Recently, the CDF collaboration has reported the result of a new W boson mass measurement with unprecedented precision [1]

$$80,433.5 \pm 9.4 \text{ MeV}, \tag{1}$$

using 8.8 fb^{-1} data collected at the Fermilab Tevatron collider with a center-of-mass energy of 1.96 TeV. Comparing with the SM expectation of $80,357 \pm 6$ MeV [2], the new measurement of the W boson mass suggests a difference with a significance of 7.0σ. Performing a global fit of electroweak data together with

[*]dongwon.jung@yonsei.ac.kr
[†]yongtae1heo@gmail.com
[‡]jslee@jnu.ac.kr

the high-precision CDF measurement while fixing $U = 0$, one may find the large central values of the oblique parameters S and T together with the standard deviations such as [3]

$$(\hat{S}_0, \sigma_S) = (0.15, 0.08), \qquad (\hat{T}_0, \sigma_T) = (0.27, 0.06), \tag{2}$$

and a strong correlation $\rho_{ST} = 0.93$ between them.

Previously, by analyzing the large deviation of the S and T parameters from their SM values of zero in the framework of two Higgs doublet model (2HDM), we reported the existence of the upper limit of about 1 TeV on the masses of the heavy charged and neutral Higgs bosons [4].

To be specific, we take the CP-conserving (CPC) 2HDM Higgs potential and identify the lighter CP-even neutral Higgs boson as the SM-like one discovered at the LHC. Observing that the mass difference between the charged Higgs boson $H^\pm$ and the CP-odd neutral one A is required to achieve the sizable positive central value of the T parameter, we derive the upper limit on the masses of heavy Higgs bosons by combining the mass difference with the theoretical constraints on the quartic couplings of the

Higgs potential from the perturbative unitarity and for the Higgs potential to be bounded from below. Quantitatively, we present our estimation that $M_{H^\pm} \lesssim 1,000^{-100}_{+400}$ GeV taking $\hat{T}_0 = 0.27 \pm 0.06$ in the alignment limit where the lighter CP-even neutral Higgs boson behaves exactly as the SM Higgs boson [4]. We note that similar results have been obtained by the authors of Ref. [5]. For other relevant studies of the CDF W-mass anomaly in the framework of 2HDM, we refer to Refs. [3,5–25].

In this work, compared to our previous study [4], we extend our analysis by considering the Higgs potential with explicit CP violation. In the presence of CP-violating (CPV) phases in the Higgs potential, one cannot specify the neutral Higgs bosons according to their CP parities as in the CPC case and, instead, we have the three CP-mixed mass eigenstates of H_1, H_2, and H_3. Therefore, the observation made in the CPC case based on the mass difference between the charged Higgs boson and the CP-odd neutral one does fail and one needs the corresponding condition in the CPV case. By identifying the lightest neutral Higgs boson H_1 as the SM-like one, we find that it is necessary to have the mass splitting between the charged Higgs boson $H^\pm$ and the second heaviest neutral Higgs boson H_2 to accommodate the large positive value of the T parameter. And we improve our previous study taking account of the effects of deviation from the alignment limit and the mass splitting between the heavy neutral Higgs bosons. Through the more comprehensive and improved

analysis, we have fully figured out all the physics origins relevant for the mass scale of heavy Higgs bosons and suggest the two specific types of the mass spectrum of them. We also address the situation in which the current CDF W-mass anomaly is ameliorated to make our analysis more convincing and our results less restrictive.

This paper is organized as follows. Section II is devoted to a brief review of the 2HDM Higgs potential in the Higgs basis with explicit CP violation. In Sec. III, we elaborate on the constraints from the perturbative unitarity, the Higgs potential bounded from below, and the electroweak precision observables. In Sec. IV, we provide the comprehensive analysis why the mass splitting between the charged and the second heaviest neutral Higgs bosons is necessary and why the masses of the heavy Higgs bosons should be bounded from above. In Sec. V, we show how the mass scale of the heavy Higgs bosons behaves according to the variation of the central values of the S and T parameters and propose some benchmarking scenarios for the searches of heavy Higgs bosons at future colliders. A brief summary and conclusions are made in Sec. VI.

II. FRAMEWORK

The general 2HDM scalar potential in the so-called Higgs basis [26,27] where only one doublet contains the nonvanishing vacuum expectation value v is given by [28]

$$
\begin{aligned}
V_{\mathcal{H}} =\ & Y_1(\mathcal{H}_1^\dagger \mathcal{H}_1) + Y_2(\mathcal{H}_2^\dagger \mathcal{H}_2) + Y_3(\mathcal{H}_1^\dagger \mathcal{H}_2) + Y_3^*(\mathcal{H}_2^\dagger \mathcal{H}_1) + Z_1(\mathcal{H}_1^\dagger \mathcal{H}_1)^2 + Z_2(\mathcal{H}_2^\dagger \mathcal{H}_2)^2 + Z_3(\mathcal{H}_1^\dagger \mathcal{H}_1)(\mathcal{H}_2^\dagger \mathcal{H}_2) \\
& + Z_4(\mathcal{H}_1^\dagger \mathcal{H}_2)(\mathcal{H}_2^\dagger \mathcal{H}_1) + Z_5(\mathcal{H}_1^\dagger \mathcal{H}_2)^2 + Z_5^*(\mathcal{H}_2^\dagger \mathcal{H}_1)^2 + Z_6(\mathcal{H}_1^\dagger \mathcal{H}_1)(\mathcal{H}_1^\dagger \mathcal{H}_2) + Z_6^*(\mathcal{H}_1^\dagger \mathcal{H}_1)(\mathcal{H}_2^\dagger \mathcal{H}_1) \\
& + Z_7(\mathcal{H}_2^\dagger \mathcal{H}_2)(\mathcal{H}_1^\dagger \mathcal{H}_2) + Z_7^*(\mathcal{H}_2^\dagger \mathcal{H}_2)(\mathcal{H}_2^\dagger \mathcal{H}_1),
\end{aligned}
\tag{3}
$$

which contains 3 dimensionful quadratic and 7 dimensionless quartic parameters of which four parameters of Y_3 and $Z_{5,6,7}$ are complex. The complex $SU(2)_L$ doublets of $\mathcal{H}_1$ and $\mathcal{H}_2$ can be parametrized as

$$
\mathcal{H}_1 = \begin{pmatrix} G^+ \\ \frac{1}{\sqrt{2}}(v + \varphi_1 + iG^0) \end{pmatrix}; \quad \mathcal{H}_2 = \begin{pmatrix} H^+ \\ \frac{1}{\sqrt{2}}(\varphi_2 + ia) \end{pmatrix}, \tag{4}
$$

where $v = (\sqrt{2}G_F)^{-1/2} \simeq 246.22$ GeV and $G^{\pm,0}$ and $H^\pm$ stand for the Goldstone and charged Higgs bosons, respectively. For the neutral Higgs bosons, the CP-odd state a and the two CP-even states φ_1 and φ_2 result in three CP-mixed mass eigenstates $H_{1,2,3}$ through mixing and one of them should play the role of the SM Higgs boson. The tadpole conditions relate the quadratic parameters Y_1 and Y_3 to Z_1 and Z_6, respectively, as follows:

$$
Y_1 + Z_1 v^2 = 0; \qquad Y_3 + \frac{1}{2}Z_6 v^2 = 0. \tag{5}
$$

The 2HDM Higgs potential includes the mass terms which can be cast into the form consisting of two parts

$$
V_{\mathcal{H},\text{mass}} = M_{H^\pm}^2 H^+ H^- + \frac{1}{2}(\varphi_1\, \varphi_2\, a)\mathcal{M}_0^2 \begin{pmatrix} \varphi_1 \\ \varphi_2 \\ a \end{pmatrix}, \tag{6}
$$

in terms of the charged Higgs bosons $H^\pm$, the neutral CP-even Higgs bosons $\varphi_{1,2}$, and the neutral CP-odd Higgs boson a. The charged Higgs boson mass is given by

$$
M_{H^\pm}^2 = Y_2 + \frac{1}{2}Z_3 v^2, \tag{7}
$$

while the 3×3 mass-squared matrix of the neutral Higgs bosons $\mathcal{M}_0^2$ takes the form

$$\mathcal{M}_0^2 = \begin{pmatrix} 0 & 0 & 0 \\ 0 & M_A^2 & 0 \\ 0 & 0 & M_A^2 \end{pmatrix}$$

$$+ \begin{pmatrix} 2Z_1 & \mathfrak{Re}(Z_6) & -\mathfrak{Im}(Z_6) \\ \mathfrak{Re}(Z_6) & 2\mathfrak{Re}(Z_5) & -\mathfrak{Im}(Z_5) \\ -\mathfrak{Im}(Z_6) & -\mathfrak{Im}(Z_5) & 0 \end{pmatrix} v^2, \quad (8)$$

where $M_A^2 = M_{H^\pm}^2 + [Z_4/2 - \mathfrak{Re}(Z_5)]v^2$. Note that the quartic couplings Z_2 and Z_7 have nothing to do with the masses of Higgs bosons and the mixing of the neutral ones. We further note that φ_1 does not mix with φ_2 and a in the $Z_6 = 0$ limit and φ_2 does not mix with a if $\mathfrak{Im}Z_5 = 0$ imposed additionally. Therefore, when $Z_6 = \mathfrak{Im}Z_5 = 0$, the three states φ_1, φ_2, and a themselves constitute the three mass eigenstates and φ_1 plays the role of the SM Higgs boson.

Given the 3×3 real and symmetric mass-squared $\mathcal{M}_0^2$, one may describe the mixing among the neutral Higgs bosons by introducing the 3×3 orthogonal matrix O

$$(\varphi_1, \varphi_2, a)_\alpha^T = O_{\alpha i}(H_1, H_2, H_3)_i^T, \quad (9)$$

which satisfies the relation

$$O^T \mathcal{M}_0^2 O = \mathrm{diag}(M_{H_1}^2, M_{H_1}^2, M_{H_3}^2) \quad (10)$$

with the increasing ordering of $M_{H_1} \leq M_{H_2} \leq M_{H_3}$. When the three masses of the neutral Higgs bosons and the elements of the orthogonal mixing matrix O are given, the quartic couplings Z_1, Z_4, Z_5, and Z_6 in the neutral-Higgs-boson mass-squared matrix $\mathcal{M}_0^2$ are given by

$$Z_1 = \frac{1}{2v^2}(M_{H_1}^2 O_{\varphi_1 1}^2 + M_{H_2}^2 O_{\varphi_1 2}^2 + M_{H_3}^2 O_{\varphi_1 3}^2),$$

$$Z_4 = \frac{1}{v^2}[M_{H_1}^2(O_{\varphi_2 1}^2 + O_{a1}^2) + M_{H_2}^2(O_{\varphi_2 2}^2 + O_{a2}^2) + M_{H_3}^2(O_{\varphi_2 3}^2 + O_{a3}^2) - 2M_{H^\pm}^2],$$

$$Z_5 = \frac{1}{2v^2}[M_{H_1}^2(O_{\varphi_2 1}^2 - O_{a1}^2) + M_{H_2}^2(O_{\varphi_2 2}^2 - O_{a2}^2) + M_{H_3}^2(O_{\varphi_2 3}^2 - O_{a3}^2)]$$

$$- \frac{i}{v^2}(M_{H_1}^2 O_{\varphi_2 1} O_{a1} + M_{H_2}^2 O_{\varphi_2 2} O_{a2} + M_{H_3}^2 O_{\varphi_2 3} O_{a3}),$$

$$Z_6 = \frac{1}{v^2}(M_{H_1}^2 O_{\varphi_1 1} O_{\varphi_2 1} + M_{H_2}^2 O_{\varphi_1 2} O_{\varphi_2 2} + M_{H_3}^2 O_{\varphi_1 3} O_{\varphi_2 3})$$

$$- \frac{i}{v^2}(M_{H_1}^2 O_{\varphi_1 1} O_{a1} + M_{H_2}^2 O_{\varphi_1 2} O_{a2} + M_{H_3}^2 O_{\varphi_1 3} O_{a3}), \quad (11)$$

for given v and $M_{H^\pm}$. We observe that $\mathfrak{Im}(Z_5)$ and $\mathfrak{Im}(Z_6)$ contain the products of $O_{\varphi_2 i} O_{ai}$ and $O_{\varphi_1 i} O_{ai}$ with $i = 1, 2, 3$, respectively, each of which identically vanishes if the mass eigenstate H_i carries its own definite CP parity.

Once the mixing matrix O is given, the cubic interactions of the neutral and charged Higgs bosons with the massive vector bosons Z and $W^\pm$ are described by the following interaction Lagrangians:

$$\mathcal{L}_{HVV} = gM_W\left(W_\mu^+ W^{-\mu} + \frac{1}{2c_W^2}Z_\mu Z^\mu\right)\sum_i g_{H_iVV}H_i,$$

$$\mathcal{L}_{HHZ} = \frac{g}{2c_W}\sum_{i>j}g_{H_iH_jZ}Z^\mu(H_i\overset{\leftrightarrow}{\partial}_\mu H_j),$$

$$\mathcal{L}_{HH^\pm W^\mp} = -\frac{g}{2}\sum_i g_{H_iH^+W^-}W^{-\mu}(H_i i\overset{\leftrightarrow}{\partial}_\mu H^+) + \mathrm{H.c.}, \quad (12)$$

where $X\overset{\leftrightarrow}{\partial}_\mu Y = X\partial_\mu Y - (\partial_\mu X)Y$ and $i, j = 1, 2, 3$. Note that the normalized couplings $g_{H_iVV}, g_{H_iH_jZ}$ and $g_{H_iH^+W^-}$

are given in terms of the neutral Higgs-boson 3×3 mixing matrix O by (note that $\det(O) = \pm 1$ for any orthogonal matrix O):

$$g_{H_iVV} = O_{\varphi_1 i},$$

$$g_{H_iH_jZ} = \mathrm{sign}[\det(O)]\epsilon_{ijk}g_{H_kVV} = \mathrm{sign}[\det(O)]\epsilon_{ijk}O_{\varphi_1 k},$$

$$g_{H_iH^+W^-} = -O_{\varphi_2 i} + iO_{ai}, \quad (13)$$

leading to the following sum rules:

$$\sum_{i=1}^3 g_{H_iVV}^2 = 1 \quad \text{and} \quad g_{H_iVV}^2 + |g_{H_iH^+W^-}|^2 = 1$$

for each $i = 1, 2, 3$. (14)

Introducing the three mixing angles γ, η, and ω, the orthogonal mixing matrix O might be parametrized as follows:

$$O = O_\gamma O_\eta O_\omega \equiv \begin{pmatrix} c_\gamma & s_\gamma & 0 \\ -s_\gamma & c_\gamma & 0 \\ 0 & 0 & 1 \end{pmatrix} \begin{pmatrix} c_\eta & 0 & s_\eta \\ 0 & 1 & 0 \\ -s_\eta & 0 & c_\eta \end{pmatrix} \begin{pmatrix} 1 & 0 & 0 \\ 0 & c_\omega & s_\omega \\ 0 & -s_\omega & c_\omega \end{pmatrix}$$

$$= \begin{pmatrix} c_\gamma c_\eta & s_\gamma c_\omega - c_\gamma s_\eta s_\omega & s_\gamma s_\omega + c_\gamma s_\eta c_\omega \\ -s_\gamma c_\eta & c_\gamma c_\omega + s_\gamma s_\eta s_\omega & c_\gamma s_\omega - s_\gamma s_\eta c_\omega \\ -s_\eta & -c_\eta s_\omega & c_\eta c_\omega \end{pmatrix}. \tag{15}$$

Identifying the lightest state H_1 as the SM-like Higgs boson, one may see $g_{H_1 VV} = O_{\varphi_1 1} = c_\gamma c_\eta$ which should take the SM value of 1 in the alignment limit. Therefore, in this parameterization, the alignment limit might be realized by taking $\gamma = \eta = 0$ and one may take the convention of $|\gamma| \leq \pi/2$ and $|\eta| \leq \pi/2$ without loss of generality to have positive $g_{H_1 VV}$ both in the CPC ($\eta = 0$) and CPV ($\eta \neq 0$) cases. Note that, even in the alignment limit of $g_{H_1 VV} = 1$, the CP-even state φ_2 and the CP-odd one a mix to result in the two heavy states H_2 and H_3 and the mixing between φ_2 and a is described by the CPV mixing angle ω. Incidentally, by taking $\gamma = \eta = 0$ in the alignment limit, we have

$$Z_1|_{\gamma=\eta=0} = \frac{M_{H_1}^2}{2v^2}, \qquad Z_4|_{\gamma=\eta=0} = \frac{M_{H_2}^2 + M_{H_3}^2 - 2M_{H^\pm}^2}{v^2},$$

$$Z_6|_{\gamma=\eta=0} = 0,$$

$$Z_5|_{\gamma=\eta=0} = -\frac{M_{H_3}^2 - M_{H_2}^2}{2v^2} c_{2\omega} - i \frac{M_{H_3}^2 - M_{H_2}^2}{2v^2} s_{2\omega}. \tag{16}$$

In the CPC alignment limit of $s_{2\omega} = 0$, H_2 (H_3) is CP odd when $|s_\omega| = 1$ ($|c_\omega| = 1$). We observe that the upper limits on the absolute values of the quartic couplings Z_4 and Z_5 constrain the product of the mass scale of heavy Higgs bosons and the mass splitting between them. For example, in the alignment limit, the upper limit on $|Z_5|$ puts the following constraint on the mass splitting between the heavy neutral Higgs bosons:

$$M_{H_3} - M_{H_2} \leq \frac{2|Z_5|_{\max} v^2}{M_{H_3} + M_{H_2}}, \tag{17}$$

which leads to the more degenerate mass spectrum of the two heavy neutral Higgs bosons as they become heavier.

The Higgs potential contains 3 dimensionful quadratic parameters $Y_{1,2,3}$ and 7 dimensionless quartic parameters Z_{1-7}, see Eq. (3). Using the tadpole conditions given by Eq. (5), the parameters Y_1 and Y_3 might be removed in favor of v, Z_1, and Z_6, and the remaining dimensionful parameter Y_2 can be removed in favor of Z_3 and $M_{H^\pm}$, see Eq. (7). This observation leads to the input parameter set

$$\mathcal{I}_Z = \{v, M_{H^\pm}; Z_1, Z_4, Z_5, Z_6; Z_3; Z_2, Z_7\}. \tag{18}$$

Alternatively, one may use the more physical set of input parameters

$$\mathcal{I}_P = \{v, M_{H^\pm}; M_{H_1}, M_{H_2}, M_{H_3}, \{O\}_{3\times3}; Z_3; Z_2, Z_7\}, \tag{19}$$

by exploiting the relations given by Eq. (11). In either of the two sets, there are three parameters involved with CP violation: $\Im m(Z_5)$, $\Im m(Z_6)$, and $\Im m(Z_7)$ in $\mathcal{I}_Z$ or η, ω, and $\Im m(Z_7)$ in $\mathcal{I}_P$. But one should be cautious to note that the three CPV parameters are not all physical and physical observables depend on only two (combinations) of them. This could be understood by observing that the Higgs potential is invariant under the following phase rotations:

$$\mathcal{H}_2 \to e^{+i\zeta} \mathcal{H}_2; \qquad Z_5 \to Z_5 e^{-2i\zeta},$$

$$Z_6 \to Z_6 e^{-i\zeta}, \qquad Z_7 \to Z_7 e^{-i\zeta}, \tag{20}$$

which lead to the following two rephasing-invariant CPV phases

$$\theta_1 \equiv \text{Arg}[Z_6(Z_5^*)^{1/2}] \quad \text{and} \quad \theta_2 \equiv \text{Arg}[Z_7(Z_5^*)^{1/2}], \tag{21}$$

pivoting around the complex quartic coupling Z_5 [28].

Note that, under phase rotations given by Eq. (20), the 3×3 mass-squared matrix $\mathcal{M}_0^2$ of the neutral Higgs bosons transforms also and, accordingly, the mixing matrix O is shifted [29,30]. More precisely, for the convention given by Eqs. (9) and (10) adopted in this work, the phase rotation $\mathcal{H}_2 \to e^{i\zeta} \mathcal{H}_2$ or $(\varphi_1, \varphi_2, a)^T \to O_\zeta^T (\varphi_1, \varphi_2, a)^T$ leads to [28]

$$\mathcal{M}_0^2 \to O_\zeta^T \mathcal{M}_0^2 O_\zeta; \qquad O \to O_\zeta^T O, \tag{22}$$

with

$$O_\zeta = \begin{pmatrix} 1 & 0 & 0 \\ 0 & c_\zeta & s_\zeta \\ 0 & -s_\zeta & c_\zeta \end{pmatrix}. \tag{23}$$

Exploiting this feature, one may observe that, among the three mixing angles of γ, η, and ω parametrizing the mixing matrix O as in Eq. (15), the two CPV angles η and ω are not always independent. For example, one may take the input parameter set $\mathcal{I}_Z$ and choose the basis in which $\Im m(Z_5) = 0$ by an appropriate phase rotation. In this case, one may extract the three mixing angles γ, η, and ω by diagonalizing

the 3×3 mass-squared matrix $\mathcal{M}_0^2$ given by Eq. (8). But, note that the two CPV angles η and ω cannot be independent since CP violation in the neutral Higgs sector is dictated solely by $\Im m(Z_6)$ in this case with $\Im m(Z_5) = 0$.[1] In fact, using Eqs. (11) and (15), one may see that they are related through the following relation

$$\Im m(Z_5) = \left[\frac{M_{H_3}^2 c_\omega^2 + M_{H_2}^2 s_\omega^2 - M_{H_1}^2}{v^2} s_\gamma s_\eta \right.$$
$$\left. - \frac{M_{H_3}^2 - M_{H_2}^2}{v^2} c_\gamma c_\omega s_\omega \right] c_\eta = 0, \qquad (24)$$

which can be solved for s_η when $c_\eta \neq 0$ [28]:

$$s_\eta|_{\Im m Z_5 = 0} = \frac{(M_{H_3}^2 - M_{H_2}^2) c_\gamma c_\omega s_\omega}{(M_{H_3}^2 c_\omega^2 + M_{H_2}^2 s_\omega^2 - M_{H_1}^2) s_\gamma}. \qquad (25)$$

Of course, one may choose the basis in which both $\Im m(Z_5)$ and $\Im m(Z_6)$ are nonvanishing. In this case, η and ω are independent from each other though the physical observables such as the masses of the neutral Higgs bosons and their couplings to two massive vector bosons depend only on the relative phase $\theta_1 = \text{Arg}[Z_6(Z_5^*)^{1/2}]$ which is invariant under the phase rotations given by Eq. (20).

In the left panel of Fig. 1, we show the masses of three neutral Higgs bosons M_{H_i} and their couplings to two massive vector bosons $g_{H_i VV}$ as functions of $\theta_1 = \phi_6 - \phi_5/2$ taking $Z_1 = 0.13$, $Z_3 = 2.5$, $Z_4 = 3.0$, $|Z_5| = |Z_6| = 0.5$, and $M_{H^\pm} = 500$ GeV while varying $\phi_5 \equiv \text{Arg}(Z_5)$ and $\phi_6 \equiv \text{Arg}(Z_6)$ from $-\pi$ to π.[2] We observe that the physical observables shown depend only on the rephasing-invariant CPV phase of θ_1. Note that Z_7 is not involved with the masses and mixing of the charged and neutral Higgs bosons and, in this case, there is only one physical CPV phase of θ_1. On the other hand, as will be addressed soon in the next section, the perturbative unitarity conditions and those for the Higgs potential to be bounded from below involve all the seven quartic couplings Z_{1-7} and, in this case, there are two physical CPV phases of θ_1 and $\theta_2 = \phi_7 - \phi_5/2$ with $\phi_7 \equiv \text{Arg}(Z_7)$. In the right panel of Fig. 1, we show the region on the $\phi_7 - \phi_6$ plane in

which the two conditions are fulfilled taking $Z_1 = 0.13$, $Z_2 = 0.5$, $Z_3 = 2.5$, $Z_4 = 3.0$, and $|Z_5| = |Z_6| = |Z_7| = 0.5$ while varying ϕ_6 and ϕ_7 from $-\pi$ to π. For ϕ_5, we have taken the four representative values of $-\pi$, $-\pi/2$, 0, and $\pi/2$.[3] We observe that the allowed regions shift along the $\phi_6 = \phi_7$ line by the amount of $\phi_5/2$ as they should do. Incidentally, we also explicitly check the relation Eq. (25) in the subset of the parameter space in which $\Im m(Z_5) = 0$ and $c_\eta \neq 0$ by choosing the input parameter set $\mathcal{I}_Z$ while scanning all the three CPV potential parameters of $\Im m(Z_5)$, $\Im m(Z_6)$, and $\Im m(Z_7)$ redundantly.

For our study, we choose the set $\mathcal{I}_P$ given by Eq. (19) for the input parameters:

$$\mathcal{I}_P = \{v, M_{H^\pm}; M_{H_1}, M_{H_2}, M_{H_3}, \{O\}_{3\times3}; Z_3; Z_2, Z_7\},$$

with $\{O\}_{3\times3} = \gamma, \eta, \omega$. The set $\mathcal{I}_P$ contains 12 real degrees of freedom including v. For the angles γ and η, we take the convention of $|\gamma| \leq \pi/2$ and $|\eta| \leq \pi/2$ without loss of generality resulting in $c_\gamma \geq 0$ and $c_\eta \geq 0$ and the angle ω is varied between $-\pi$ to π. We identify lightest neutral Higgs boson H_1 as the SM-like one with $M_{H_1} = 125.5$ GeV and the heavy Higgs masses squared are scanned up to $(1.5 \text{ TeV})^2$. Finally, the quartic couplings Z_2, $|Z_3|$, $|\Re e(Z_7)|$, and $|\Im m(Z_7)|$ are scanned up to 3, 10, 5, respectively.[4] Though our choice of parameters is redundant considering the rephasing invariance of the Higgs potential under the phase rotations given by Eq. (20), it should be useful for checking the rephasing invariance and the consistency of our numerical analysis explicitly.

III. CONSTRAINTS

First, we consider the perturbative unitarity (UNIT) conditions and those for the Higgs potential to be bounded from below (BFB) to obtain the primary theoretical constraints on the potential parameters or, equivalently, the constraints on the Higgs-boson masses and the three mixing angles including correlations among them. The unitarity conditions in the most general 2HDM have been investigated in Refs. [31–33]. On the other hand, the necessary and sufficient conditions for the 2HDM potential to be bounded from below have been derived in Refs. [34–37]. Recently, the authors of Ref. [38] have provided some analytic expressions for the UNIT and BFB conditions in the most general 2HDM. In this work, for the unitarity conditions, we closely follow Ref. [33] taking into account three scattering matrices which are expressed in terms of the quartic couplings Z_{1-7}. Using the set $\mathcal{I}_P$ in Eq. (19) for the

---

[1]It is worthwhile to note that this is the direct consequence of the tree-level analysis of the Higgs potential. Beyond the tree level, the 3×3 mass-squared matrix $\mathcal{M}_0^2$ might receive additional CPV contributions coming from other than $\Im m(Z_5)$ and $\Im m(Z_6)$ through higher loop corrections. In the 2HDM framework, the additional CPV sources include $\Im m(Z_7)$ and $\Im m(\zeta_{u,d,e})$ with the latter ones possibly residing in the Yukawa sector, see Eq. (35) and discussion below. Regarding the rephasing invariance of all the relevant CPV phases, we refer to Ref. [28].

[2]Note that varying ϕ_5 and ϕ_6 separately is redundant considering the rephasing invariance of the Higgs potential. But, it serves for our purpose here to check that the physical observables under consideration indeed depend on the rephasing-invariant CPV phase of θ_1 only.

[3]Note again that varying ϕ_5, ϕ_6, and ϕ_7 separately is redundant considering the rephasing invariance of the Higgs potential. But, it serves for our purpose here to check that the physical conditions under consideration indeed depend only on the two rephasing-invariant CPV phases of θ_1 and θ_2.

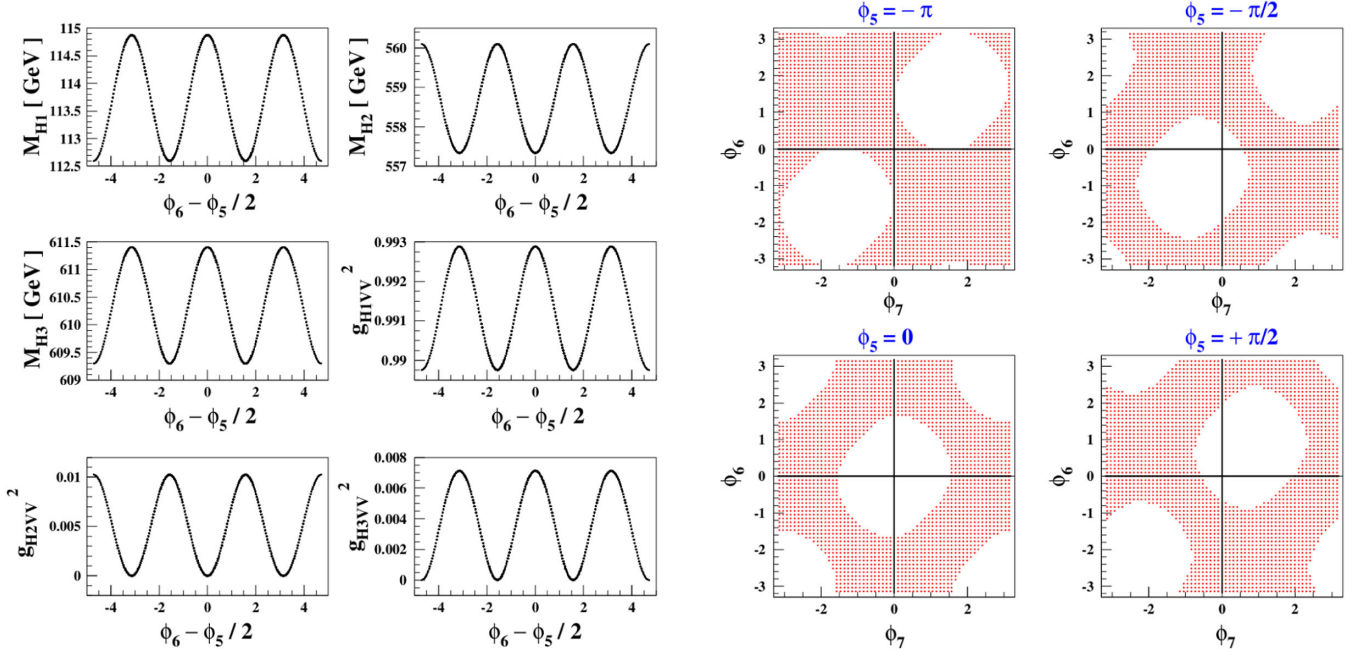[4]Note that $Z_2 \geq 0$, see Eq. (26).

FIG. 1.   Left: the masses of three neutral Higgs bosons M_{H_i} and their couplings-squared to two massive vector bosons g_{H_iVV} as functions of $\theta_1 = \phi_6 - \phi_5/2$ taking $Z_1 = 0.13$, $Z_3 = 2.5$, $Z_4 = 3.0$, $|Z_5| = |Z_6| = 0.5$, and $M_{H^\pm} = 500$ GeV while varying $\phi_5 \equiv \mathrm{Arg}(Z_5)$ and $\phi_6 \equiv \mathrm{Arg}(Z_6)$ from $-\pi$ to π. Right: the allowed region on the $\phi_7 - \phi_6$ plane obtained by imposing the UNIT $\oplus$ BFB constraints for the four values of $\phi_5 = -\pi$ (upper-left), $-\pi/2$ (upper-right), 0 (lower-left), and $\pi/2$ (lower-right). The quartic couplings are taken as in the left panel additionally with $Z_2 = 0.5$ and $|Z_7| = 0.5$.

input parameters, all the seven quartic couplings are fixed exploiting the relations in Eq. (11). For the details of the implementation of the UNIT conditions, we refer to Refs. [28,33]. For the BFB constraints, we require the following five necessary conditions for the Higgs potential to be bounded-from-below [39]:

$$Z_1 \geq 0, \qquad Z_2 \geq 0;$$
$$2\sqrt{Z_1 Z_2} + Z_3 \geq 0, \qquad 2\sqrt{Z_1 Z_2} + Z_3 + Z_4 - 2|Z_5| \geq 0;$$
$$Z_1 + Z_2 + Z_3 + Z_4 + 2|Z_5| - 2|Z_6 + Z_7| \geq 0. \qquad (26)$$

Note that the first 4 inequalities are necessary and sufficient conditions when $Z_6 = Z_7 = 0$. Otherwise, they constitute only the necessary conditions together with the last one. The authors of Ref. [33] numerically analyze the BFB conditions when Z_6 and Z_7 are nonzero and complex and confirm that the five inequalities always hold at tree level. We have explicitly checked that the parameter space where the five

inequalities hold fully contains the parameter space in which the necessary and sufficient BFB conditions are fulfilled.

Second, we consider the electroweak (ELW) oblique corrections to the so-called S, T, and U parameters [40,41] which provide significant constraints on the quartic couplings of the 2HDM. Fixing $U = 0$ which is suppressed by an additional factor M_Z^2/M_{BSM}^2 [5] relative to S and T, the S and T parameters are constrained as follows [2,42]

$$\frac{(S - \hat{S}_0)^2}{\sigma_S^2} + \frac{(T - \hat{T}_0)^2}{\sigma_T^2} - 2\rho_{ST}\frac{(S - \hat{S}_0)(T - \hat{T}_0)}{\sigma_S \sigma_T}$$
$$\leq R^2(1 - \rho_{ST}^2), \qquad (27)$$

with $R^2 = 2.3, 4.61, 5.99, 9.21, 11.83$ at 68.3%, 90%, 95%, 99%, and 99.7% confidence levels (CLs), respectively. For our numerical analysis, we take the 95% CL limit. For the central values $\hat{S}_0$ and $\hat{T}_0$, the standard deviations $\sigma_{S,T}$, and the correlations between them, we adopt [2,3]:

$$\textbf{PDG}: (\hat{S}_0, \sigma_S) = (0.00, 0.07), \qquad (\hat{T}_0, \sigma_T) = (0.05, 0.06), \qquad \rho_{ST} = 0.92,$$
$$\textbf{CDF}: (\hat{S}_0, \sigma_S) = (0.15, 0.08), \qquad (\hat{T}_0, \sigma_T) = (0.27, 0.06), \qquad \rho_{ST} = 0.93. \qquad (28)$$

---

[5]Here, M_{BSM} denotes some heavy mass scale involved with new physics beyond the Standard Model (BSM).

Using the set $\mathcal{I}_P$ for the input parameters and exploiting the relations among the couplings of the Higgs bosons to the massive vector bosons given in Eq. (14), the S and T parameters might be estimated using the following expressions at the one-loop order [28,30,39,42–45][6]:

$$\frac{T}{\frac{\sqrt{2}G_F}{16\pi^2\alpha_{\text{EM}}}} = (1 - g^2_{H_1VV})F_\Delta(M_{H_1}, M_{H^\pm}) + (1 - g^2_{H_2VV})F_\Delta(M_{H_2}, M_{H^\pm}) + (1 - g^2_{H_3VV})F_\Delta(M_{H_3}, M_{H^\pm})$$

$$- g^2_{H_3VV}F_\Delta(M_{H_1}, M_{H_2}) - g^2_{H_2VV}F_\Delta(M_{H_1}, M_{H_3}) - g^2_{H_1VV}F_\Delta(M_{H_2}, M_{H_3}),$$

$$4\pi S = -F'_\Delta(M_{H^\pm}, M_{H^\pm}) + g^2_{H_3VV}F'_\Delta(M_{H_1}, M_{H_2}) + g^2_{H_2VV}F'_\Delta(M_{H_1}, M_{H_3}) + g^2_{H_1VV}F'_\Delta(M_{H_2}, M_{H_3}), \qquad (29)$$

where the one-loop functions are given by

$$F_\Delta(m_0, m_1) = F_\Delta(m_1, m_0) = \frac{m_0^2 + m_1^2}{2} - \frac{m_0^2 m_1^2}{m_0^2 - m_1^2}\ln\frac{m_0^2}{m_1^2},$$

$$F'_\Delta(m_0, m_1) = F'_\Delta(m_1, m_0) = -\frac{1}{3}\left[\frac{4}{3} - \frac{m_0^2\ln m_0^2 - m_1^2\ln m_1^2}{m_0^2 - m_1^2} - \frac{m_0^2 + m_1^2}{(m_0^2 - m_1^2)^2}F_\Delta(m_0, m_1)\right]. \qquad (30)$$

When the BSM Higgs bosons are almost degenerate and they are much heavier than the SM-like one, it is useful to know the asymptotic behavior of the one-loop functions. When $m_0 \sim m_1$, we find[7]

$$F_\Delta(m_0, m_1) = \frac{2(m_0 - m_1)^2}{3} - \frac{2(m_0 - m_1)^4}{15(m_0 + m_1)^2} + \mathcal{O}\left[\frac{(m_0 - m_1)^6}{(m_0 + m_1)^4}\right],$$

$$F'_\Delta(m_0, m_1) = \frac{1}{3}\ln\left[\frac{(m_0 + m_1)^2}{4}\right] + \frac{(m_0 - m_1)^2}{5(m_0 + m_1)^2} + \mathcal{O}\left[\frac{(m_0 - m_1)^4}{(m_0 + m_1)^4}\right]. \qquad (31)$$

On the other hand, for $m_1 \gg m_0$, we have

$$F_\Delta(m_0, m_1) = \frac{m_1^2}{2} + \left(\frac{1}{2} + \ln\frac{m_0^2}{m_1^2}\right)m_0^2 + \mathcal{O}\left[\left(\frac{m_0^4}{m_1^2}\right)\ln\frac{m_0^2}{m_1^2}\right],$$

$$F'_\Delta(m_0, m_1) = \frac{\ln m_1^2}{3} - \frac{5}{18} + \frac{2m_0^2}{3m_1^2} + \mathcal{O}\left[\left(\frac{m_0^4}{m_1^4}\right)\ln\frac{m_0^2}{m_1^2}\right]. \qquad (32)$$

In the alignment limit where $g^2_{H_1VV} = 1$ and $g^2_{H_2VV} = g^2_{H_3VV} = 0$, we note that S and T are symmetric under the exchange $M_{H_2} \leftrightarrow M_{H_3}$ and they are identically vanishing if $M_{H_2} = M_{H_3} = M_{H^\pm}$ since $F_\Delta(m, m) = 0$ and $F'_\Delta(m, m) = \ln m^2/3$.

In the upper-left panel of Fig. 2, we show the two ELW ellipses which delimit the CDF (upper ellipse) and PDG (lower ellipse) 95% CL regions on the $S - T$ plane, see Eqs. (27) and (28). The scattered region in each of them has been obtained by imposing the UNIT and *necessary* BFB constraints as well as the ELW one as indicated by the abbreviation UNIT $\oplus$ BFB $\oplus$ ELW$_{95\%}$ in the figure caption. We magnify the CDF and PDG regions in the

upper-right and lower-left panels, respectively, with the colored dots for $M_{H^\pm} > M_{H_1}$ (black + red + blue), $M_{H^\pm} > 500$ GeV (red + blue), and $M_{H^\pm} > 900$ GeV (blue). We observe that $M_{H^\pm}$ is smaller than 900 GeV for CDF when S is positive, see the upper-right panel. In the lower-right plane, we show the two magnified CDF and PDG regions together for simultaneous comparisons. We find that S takes values in the range between -0.03 and 0.05 whose absolute values are smaller than $\sigma_S = 0.07$ (PDG) and 0.08 (CDF), see Eq. (28). The T parameter takes its value between 0.12 and 0.24 (CDF) and between -0.02 and 0.14 (PDG). Note that, for CDF, the narrow region around $S = 0$ with radius about 0.005 is not allowed, see the upper-right panel. Also note that T is positive definite and sizable.

In Fig. 3, we show the normalized distributions (magenta) of the seven quartic couplings, the three mixing angles, and the masses of heavy Higgs bosons using the CDF values for $\hat{T}_0$, $\hat{S}_0$, σ_S, σ_T, and ρ_{ST}, see Eq. (28). The combined UNIT $\oplus$ BFB $\oplus$ ELW$_{95\%}$ constraints have been imposed. Also shown are the distributions (blue) requiring only the UNIT $\oplus$ BFB conditions. We find that the distributions of the real and imaginary parts of $Z_{5,6,7}$ are (almost) symmetric around 0. Meanwhile, the Z_4 distribution changes drastically to exclude the region $|Z_4| \lesssim 1$ after imposing the ELW constraint additionally. Quantitatively, we find that the quartic couplings are constrained as:

---

[6]To obtain the expressions for the T and S parameter, we use the coupling relations $g^2_{H_iH_jV} = |\epsilon_{ijk}|g^2_{H_kVV}$ and the sum rule $|g_{H_iH^+W^-}|^2 = 1 - g^2_{H_iVV}$ for $i, j = 1, 2, 3$, see Eqs. (13) and (14).

[7]Note that the one-loop functions $F_\Delta(m_0, m_1)$ and $F'_\Delta(m_0, m_1)$ are symmetric under the exchange $m_0 \leftrightarrow m_1$.
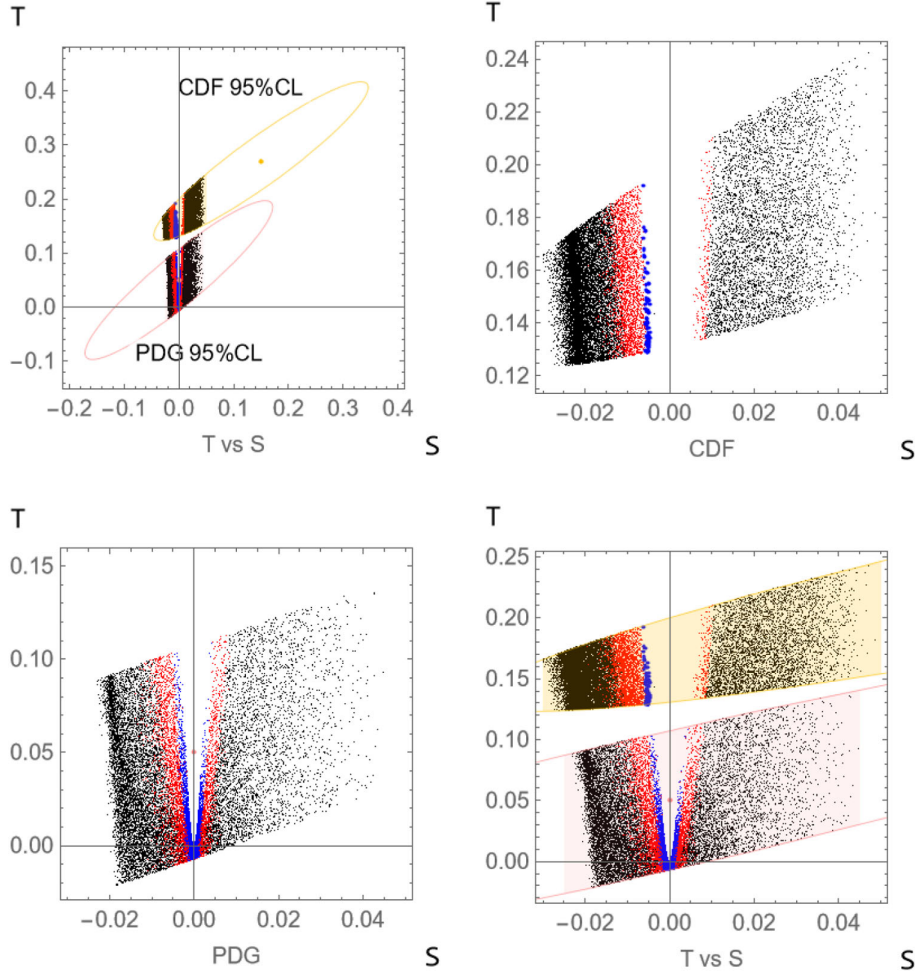
FIG. 2.   CDF and PDG: T versus S. The scattered regions are obtained by imposing the combined UNIT $\oplus$ BFB $\oplus$ ELW$_{95\%}$ constraints and the colored dots are for $M_{H^{\pm}} > M_{H_1}$ (black + red + blue), $M_{H^{\pm}} > 500$ GeV (red + blue), and $M_{H^{\pm}} > 900$ GeV (blue).

$$0.1 \lesssim Z_1 \lesssim 2.0, \qquad 0 \lesssim Z_2 \lesssim 2.1, \qquad -2.6 \lesssim Z_3 \lesssim 8.0,$$

$$-6.3 \lesssim Z_4 \lesssim -0.8 \cup 1.1 \lesssim Z_4 \lesssim 5.4,$$

$$|Z_5| \lesssim 1.7, \qquad |Z_6| \lesssim 2.4, \qquad |Z_7| \lesssim 2.7. \qquad (33)$$

The mixing angles γ and η prefer the values near to 0 while the ω distribution is flat. From the distributions of the masses of heavy Higgs bosons, we observe that the upper limit around 1 TeV emerges when the ELW constraint has been imposed in addition to the UNIT $\oplus$ BFB ones. In Fig. 3, we also show the normalized distributions (black) by picking out the points which satisfy the necessary and sufficient BFB conditions as well as the UNIT $\oplus$ ELW$_{95\%}$ constraints. We observe that the stronger BFB conditions shift the negative edge of Z_4 to the positive direction a little bit and reduce the ranges of Z_6 and Z_7 couplings as $|Z_{6,7}| \lesssim 1.9$ and strengthen the upper limit on $M_{H^{\pm},H_{2,3}}$ by the amount of about 100 GeV. Otherwise, the distributions remain the same more or less especially with the gap around $Z_4 = 0$ unaffected.

In Fig. 4, we show the correlations between the heavy Higgs masses $M_{H^{\pm}}$ and M_{H_2} (upper left), $M_{H^{\pm}}$ and M_{H_3} (upper right), and M_{H_3} and M_{H_2} (lower left), and that between the mass differences $M_{H_2} - M_{H^{\pm}}$ and $M_{H_3} - M_{H_2}$ (lower right) using the CDF data, see Eq. (28). As in Fig. 3, the combined UNIT $\oplus$ BFB $\oplus$ ELW$_{95\%}$ constraints have been imposed (magenta) and the results obtained by adopting the necessary and sufficient BFB conditions are shown in black. The blue points are again for the case only with the UNIT and necessary BFB constraints. In the upper-left and lower-right panels, it is clearly shown that there should be sizable mass difference between the charged Higgs boson $H^{\pm}$ and the second heaviest neutral one H_2 to accommodate the CDF W-mass anomaly. Further we observe that, the upper limits of about 1 TeV and 900 GeV on the heaviest states emerge when $M_{H^{\pm}} > M_{H_2}$ and $M_{H^{\pm}} < M_{H_2}$, respectively. Note that, when $M_{H^{\pm}} < M_{H_2}$, the mass splitting between $H^{\pm}$ and H_2 also implies the mass splitting between $H^{\pm}$ and H_3 since $M_{H_2} < M_{H_3}$ by definition. On the other hand, when $M_{H^{\pm}} > M_{H_2}$, the heaviest neutral
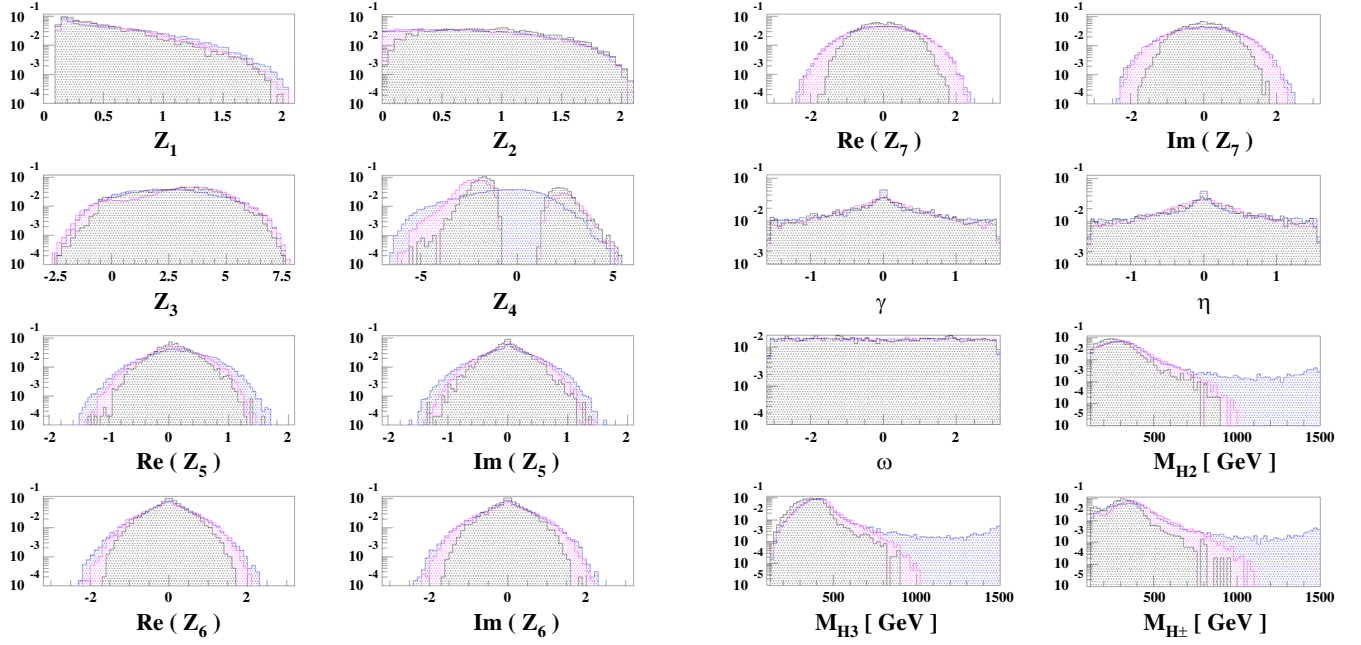
FIG. 3.   CDF: The normalized distributions of the quartic couplings, the mixing angles, and the masses of heavy Higgs bosons imposing the combined UNIT $\oplus$ BFB $\oplus$ ELW$_{95\%}$ constraints (magenta) and using the set $\mathcal{I}_P$ of the input parameters, see Eq. (19). The normalized distributions obtained by replacing the necessary BFB conditions with the necessary and sufficient ones are shown in black. For comparisons, we also show the results obtained by imposing only the UNIT and necessary BFB constraints (blue).

Higgs boson could be either heavier or lighter than the charged Higgs boson, see the upper-right panel of Fig. 4. Incidentally, we observe the mass splitting between the two heavy neutral Higgs bosons limited to be smaller than about

350 (240) GeV when $M_{H^\pm} > (<) M_{H_2}$, see the lower-right panel of Fig. 4. When the masses of the heavy Higgs bosons saturate their upper limits, there are two types of the heavy-Higgs mass spectrum given by

$$M_{H^\pm} > M_{H_2}: \; M_{H_2} \simeq M_{H_3} \simeq 1000(900) \text{ GeV}, \qquad M_{H^\pm} \simeq 1100(1000) \text{ GeV};$$
$$M_{H^\pm} < M_{H_2}: \; M_{H_2} \simeq M_{H_3} \simeq 900 \text{ GeV}, \qquad M_{H^\pm} \simeq 800 \text{ GeV}, \tag{34}$$

where the numbers in parentheses when $M_{H^\pm} > M_{H_2}$ are for the case with the necessary and sufficient BFB conditions, see the black points in Fig. 4. When $M_{H^\pm} < M_{H_2}$, we observe that the mass spectrum of heavy Higgs bosons is insensitive to the choice of the BFB conditions.

In this work, we analyze the mass spectrum of heavy Higgs bosons appearing in the CPV 2HDM especially when the central value of the T parameter significantly deviates from its SM value of zero as indicated by the CDF W-mass anomaly by combining it with the theoretical UNIT and BFB constraints. In this case, all the relevant parameters and couplings are fully determined by the CPV 2HDM potential only. Note that the theoretical UNIT and BFB conditions are given in terms of the seven quartic couplings Z_{1-7} and the S and T parameters are functions of the Higgs masses and the neutral Higgs couplings to a pair of massive vector bosons $g_{H_i VV} = O_{\varphi_1 i}$ only, see Eq. (29).

This makes our current analysis largely independent of the Yukawa sector.

Eventually, of course, one needs to implement a full phenomenological study of the Higgs bosons which incorporates flavor observables, the LHC Higgs precision data, the collider limits from the heavy Higgs boson searches carried out at the LHC, nonobservation of the electron and neutron electric dipole moments (EDMs), etc. But, to incorporate all the phenomenological constraints, one should specify the Yukawa sector since the constraints beyond the UNIT, BFB, and ELW ones strongly depend on the relevant Yukawa interactions. For example, the recent analysis of the radiative $b \to s\gamma$ decay within the so-called type-II 2HDM yields the 95% C.L. constraint of $M_{H^\pm} > 800$ GeV [46]. But it is well known that the strong upper limit on the charged Higgs boson mass becomes significantly weaker if different models for the Yukawa
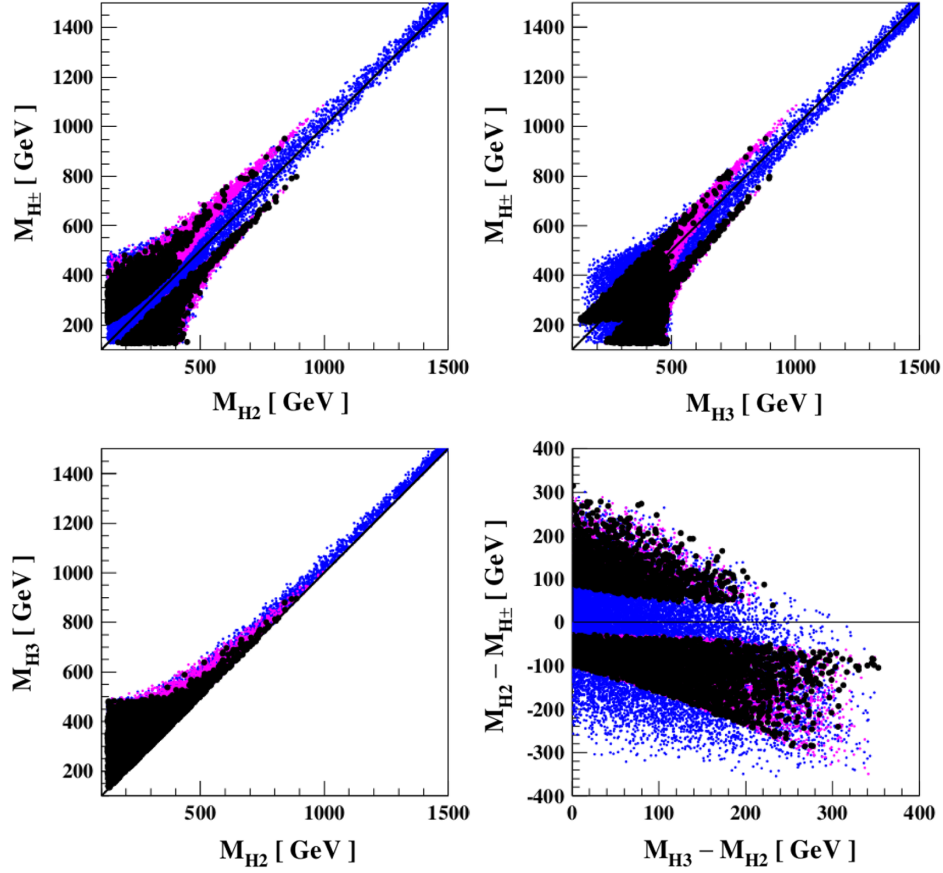
FIG. 4. CDF: Scatter plots of $M_{H^\pm}$ versus M_{H_2} (upper left), $M_{H^\pm}$ versus M_{H_3} (upper right), M_{H_3} versus M_{H_2} (lower left), and $M_{H_2} - M_{H^\pm}$ versus $M_{H_3} - M_{H_2}$ (lower right) imposing the combined UNIT $\oplus$ BFB $\oplus$ ELW$_{95\%}$ constraints (magenta) and using the set $\mathcal{I}_P$ of the input parameters, see Eq. (19). Scatter plots obtained by replacing the necessary BFB conditions with the necessary and sufficient ones are shown in black. For comparisons, we also show the results obtained by imposing only the UNIT and necessary BFB constraints (blue).

interactions are assumed. Indeed, there are wider varieties in choosing the 2HDM Yukawa sector beyond the frequently mentioned four types of 2HDM. In the 2HDM, the Yukawa couplings might be given by [28,47][8]

$$-\mathcal{L}_Y = \sum_{k=1,2} \bar{Q}_L^0 \mathbf{y}_k^u \tilde{\mathcal{H}}_k u_R^0 + \bar{Q}_L^0 \mathbf{y}_k^d \mathcal{H}_k d_R^0 + \bar{L}_L^0 \mathbf{y}_k^e \mathcal{H}_k e_R^0 + \text{H.c.},$$

(35)

which contain the six 3×3 Yukawa matrices $\mathbf{y}_{1,2}^{u,d,e}$. The Yukawa matrices of $\mathbf{y}_1^{u,d,e}$ are diagonalized to generate the masses of the SM fermions in the Higgs basis, while the Yukawa matrices of $\mathbf{y}_2^{u,d,e}$ give rise to unwanted tree-level Higgs-mediated flavor-changing neutral currents (FCNCs). To avoid the tree-level FCNC, the Glashow-Weinberg condition [48] has been usually considered leading to the conventional four types of 2HDM. But

this is not the only way to avoid the FCNC in the 2HDM. For example, one may assume the alignment of the two types of the Yukawa matrices or $\mathbf{y}_2^f = \zeta_f \mathbf{y}_1^f$ for $f = u, d, e$ by introducing the three complex alignment parameters $\zeta_{u,d,e}$ [47]. The aligned 2HDM (A2HDM) accommodates the four conventional types of 2HDM as some limiting cases when the alignment parameters are real and fully correlated [28,47].[9] Otherwise, it provides the more general 2HDM framework than the conventional ones based on the Glashow-Weinberg condition, leading to much more enriched Higgs phenomenology. For example, a very recent study shows that some LHC excesses observed by the ATLAS and CMS collaborations in their searches for heavy neutral scalars with $\tau^+\tau^-$ and $t\bar{t}$ final states are incompatible within the four conventional 2HDMs but can be accommodated within A2HDM [49]. This should imply that one needs to be very careful when interpreting experimental data if there exist several

---

[8]Here $Q_L^0 = (u_L^0, d_L^0)^T$, $L_L^0 = (\nu_L^0, e_L^0)^T$, u_R^0, d_R^0, and e_R^0 denote the electroweak eigenstates and $\tilde{\mathcal{H}}_i = i\tau_2 \mathcal{H}_i^*$.

[9]For example, the so-called type-II 2HDM can be accommodated by taking $\zeta_d = \zeta_e = -1/\zeta_u$ and $\zeta_u = 1/\tan\beta$.

theoretical frameworks available in order not to exclude regions of parameter space which could be important. A full phenomenological study of the heavy Higgs bosons including a detailed analysis of various constraints in the CPV-A2HDM framework might deserve another independent studies and, in this work, we keep our analysis independent of the Yukawa sector as much as possible.

IV. ANALYSIS

In this section, we provide the comprehensive analysis on the behavior of the masses of heavy Higgs bosons shown in Fig. 4 and investigate their dependence on the couplings of the neutral Higgs bosons to two massive vector bosons $g_{H_i VV}$ appearing in the expressions for the S and T parameters, see Eq. (29), taking account of the mass difference $M_{H_3} - M_{H_2}$. For our analysis, we adopt the necessary BFB conditions as in Eq. (26) or the magenta points in Fig. 4 for the conservative estimation of the mass spectrum of heavy Higgs bosons taking account of the limited size of our dataset and also for the easier comparisons with our previous work [4]. Otherwise, it would be understood that one might have the slightly lighter spectrum by the amount of about 100 GeV when the charged Higgs boson is the heaviest state.

The coupling of the SM-like lightest Higgs boson to two massive vector bosons, $g_{H_1 VV}$, is constrained by the precision LHC Higgs data. Denoting

$$g_{H_1 VV} \equiv 1 - \epsilon, \qquad (36)$$

the quantity ϵ is required to be smaller than about 0.05 at 1σ level [50].[10] As a measure of the deviation from the alignment limit of $g_{H_1 VV}^2 = 1$, we introduce the average coupling

$$g_{23}^2 \equiv \frac{g_{H_2 VV}^2 + g_{H_3 VV}^2}{2} = \frac{1 - g_{H_1 VV}^2}{2} = \epsilon - \frac{\epsilon^2}{2}, \quad (37)$$

which varies between 0 and 0.5 while being constrained to be smaller than about 0.05 at 1σ level by the precision LHC Higgs data.

---

[10]In Ref. [50], used are the accumulated LHC Higgs data with the integrated luminosities per experiment of approximately 5/fb at 7 TeV, 20/fb at 8 TeV, and up to 80/fb at 13 TeV. We note that there are more datasets at 13 TeV up to 139/fb and 137/fb collected with the ATLAS and CMS experiments, respectively, see Refs. [51,52]. We observe that the 1σ errors are reduced by the amount of about 30% by comparing the results presented in Ref. [51] with those in Ref. [53] in the latter the dataset up to 80/fb is used. But, without a combined ATLAS and CMS analysis, it is difficult to say conclusively how much the full 13-TeV dataset improves the measurements involved with the 125 GeV Higgs boson and, throughout this work, we use $g_{H_1 VV} \gtrsim 0.95$ as the conservative constraint on the coupling at 1σ level.

To analyze the CDF case presented in Fig. 4, we introduce the following two measures for the mass splittings of the heavy Higgs bosons:

$$\Delta \equiv M_{H_2} - M_{H^\pm}; \qquad \delta \equiv M_{H_3} - M_{H_2}, \quad (38)$$

and then the masses of heavy Higgs bosons are given by

$$M_{H^\pm} = M - \Delta/2, \qquad M_{H_2} = M + \Delta/2,$$
$$M_{H_3} = M + \Delta/2 + \delta, \qquad (39)$$

in terms of Δ, δ, and the average heavy mass scale $M = (M_{H^\pm} + M_{H_2})/2$. The quantity δ is positive definite while Δ can be either positive or negative. When $\Delta < 0$, the lightest state is H_2 while $H^\pm$ is the lightest one when $\Delta > 0$.

In Fig. 5, we show the correlations among Δ, δ, M, and g_{23}^2 imposing the combined UNIT $\oplus$ BFB $\oplus$ ELW$_{95\%}$ constraints for $\Delta < 0$ (left) and $\Delta > 0$ (right). First of all, we observe that M is constrained from the above and $|\Delta|$ is nonvanishing and sizable: $M \lesssim 1050$ GeV and $M \lesssim 850$ GeV when $\Delta < 0$ and $\Delta > 0$, respectively, and Δ converges to the values of about ± 90 GeV as M reaches its maximum values. On the other hand, the mass splitting δ between H_3 and H_2 becomes smaller as M increases as shown in Eq. (17) and H_3 could be (almost) degenerate with H_2 for the whole range of M. We further observe that $|\Delta| > \delta$ when $M > 550$ GeV, see the colored dots below (left) and above (right) the magenta lines for $|\Delta| = \delta$ in the lower-left frames. The scatter plots for M versus g_{23}^2 in the lower-right frames illustrate the effects of deviation from the alignment limit. The upper limit on M quickly decreases as g_{23}^2 deviates from the alignment limit and we find find $M \lesssim 700(600)$ GeV and $M \lesssim 600(500)$ GeV when $g_{23}^2 = 0.05(0.1)$. In this work, we concentrate on the heavy mass region with $M \gtrsim 500$ GeV where $|\Delta| \gtrsim \delta$ and, accordingly, there is a mass hierarchy such as

$$M \gg M_{H_1} \sim |\Delta| \gtrsim \delta, \qquad (40)$$

which leads to the following two types of mass spectrum

23C: $M_{H_2} < M_{H_3} < M_{H^\pm}$ when $\Delta < 0$ and $\delta < |\Delta|$;

C23: $M_{H^\pm} < M_{H_2} < M_{H_3}$ when $\Delta > 0$. $\qquad (41)$

For the 23C hierarchy, the second heaviest Higgs boson H_2 is the lightest state while the charged Higgs boson is the lightest one for the C23 hierarchy. The heaviest states are $H^\pm$ and H_3 for the 23C and C23 hierarchies, respectively.

Assuming the mass hierarchy given in Eq. (40) and keeping the leading terms for T and S using the approximations given in Eqs. (31) and (32), one may find the approximated expressions for the S and T parameters:
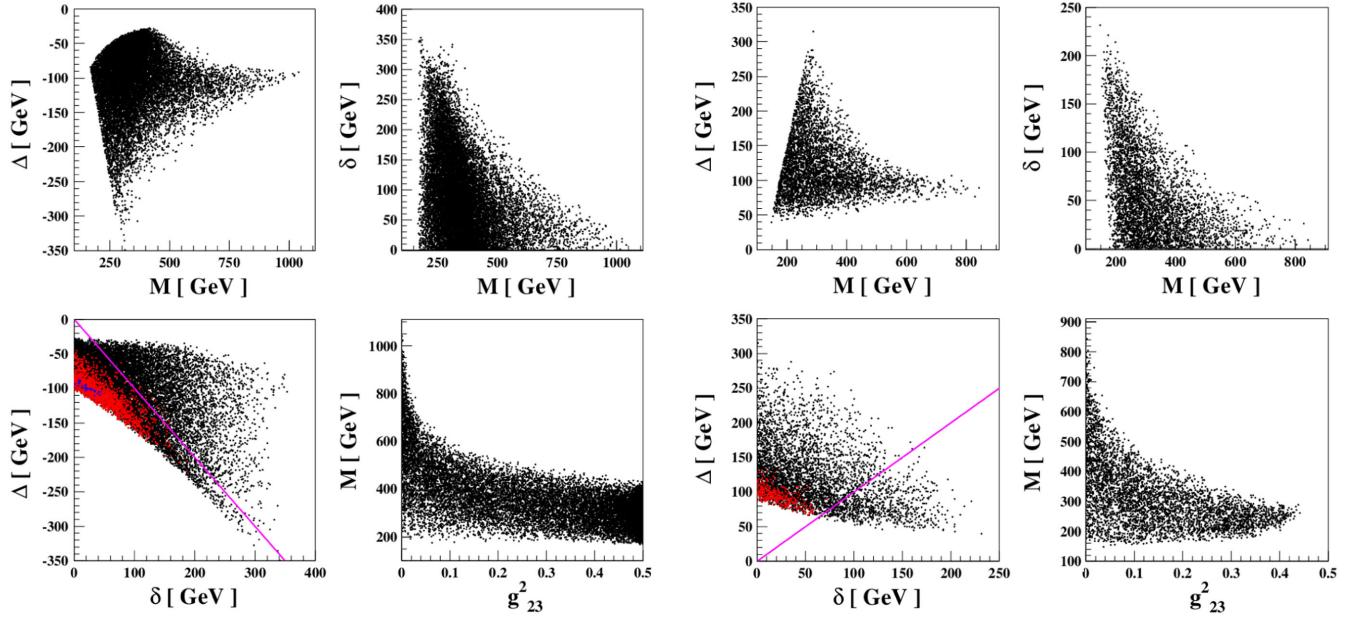
FIG. 5. CDF: (Left) Scatter plots of Δ versus M (upper left), δ versus M (upper right), Δ versus δ (lower left), and M versus g_{23}^2 (lower right) for $\Delta < 0$. [Right] The same as in the left panel but for $\Delta > 0$. The magenta lines in the lower-left frames in each panel are for $\Delta = -\delta$ (Left) and $\Delta = \delta$ (Right). And the red and blue dots are for $M > 500$ GeV (red + blue) and $M > 900$ GeV (blue), respectively. The combined UNIT $\oplus$ BFB $\oplus$ ELW$_{95\%}$ constraints are imposed.

$$\frac{T}{\frac{\sqrt{2}G_F}{16\pi^2\alpha_{\rm EM}}} \simeq \frac{4}{3}(\Delta^2 + \delta\Delta) + \left[-(2g_{23}^2\Delta + g_{H_2VV}^2\delta)M - \frac{4}{3}g_{23}^2\Delta^2 - \left(\frac{1}{2}g_{H_2VV}^2 + \frac{4}{3}g_{H_3VV}^2\right)\delta\Delta + \frac{1}{6}g_{H_2VV}^2\delta^2 \right],$$

$$4\pi S \simeq \frac{1}{3}\left(2\frac{\Delta}{M} + \frac{\delta}{M}\right) + \left[-\frac{5}{9}g_{23}^2 + \frac{1}{3}(g_{H_2VV}^2 - g_{H_3VV}^2)\frac{\delta}{M} \right], \tag{42}$$

in terms of Δ, δ, M, $g_{H_2VV}^2$, $g_{H_3VV}^2$, and g_{23}^2. Note that the quantities in the square brackets are vanishing in the alignment limit of $g_{H_2VV}^2 = g_{H_3VV}^2 = g_{23}^2 = 0$ and the terms are organized taking account of the mass hierarchy $M \gg M_{H_1} \sim |\Delta| \gtrsim \delta$, see Eq. (40). Further we observe that the terms containing either $g_{H_2VV}^2$ or $g_{H_3VV}^2$ vanish when $\delta = 0$ leaving only the terms with the average coupling g_{23}^2. One should note that T is vanishing when $\Delta = \delta = 0$ and one needs mass splittings among the heavy Higgs bosons to accommodate the sizable positive value of the T parameter. When $\delta = 0$, T still has positive contributions proportional to Δ^2 even in the alignment limit of $g_{23}^2 = 0$. When $\Delta = 0$, on the other hand, T is vanishing in the alignment and it is given by

$$\left.\frac{T}{\frac{\sqrt{2}G_F}{16\pi^2\alpha_{\rm EM}}}\right|_{\Delta=0} \simeq -g_{H_2VV}^2\delta\left(M - \frac{1}{6}\delta\right), \tag{43}$$

which is negative unless $\delta > 6M$ or identically vanishing when $g_{H_2VV} = 0$ or when H_2 is the CP-odd state. The large mass splitting between H_3 and H_2 such as $\delta > 6M$ is not allowed since it generates too large value of $|Z_5|$ violating

the perturbative UNIT constraint, see Eq. (16), let alone it is not consistent with our assumed mass hierarchy.[11] And, $T = 0$ with $g_{H_2VV} = 0$ is consistent with the observation made in the CPC case [4]: T is identically vanishing when the mass of the charged Higgs boson is equal to that of the CP-odd Higgs boson. So we conclude that, only with nonzero δ, we are heading to the opposite direction pointed by the CDF measurement of M_W and nonvanishing Δ is necessary to produce the sizable and positive definite value of the T parameter. To strengthen our claim, we extend our discussion to the case with $\Delta \neq 0$. In this case, dropping the terms suppressed by the factor Δ/M or δ/M compared to the leading term in the square bracket in Eq. (42), the expression for T is further simplified into

$$\frac{T}{\frac{\sqrt{2}G_F}{16\pi^2\alpha_{\rm EM}}} \simeq \frac{4}{3}(\Delta^2 + \delta\Delta) - (2g_{23}^2\Delta + g_{H_2VV}^2\delta)M, \tag{44}$$

---

[11]We also note that $\delta \sim 6M$ leads to $S \sim 1/2\pi$ when $\Delta = g_{23}^2 = 0$, see Eq. (42), which is far outside the scattered regions presented in Fig. 2 which are obtained by imposing the combined UNIT $\oplus$ BFB $\oplus$ ELW$_{95\%}$ constraints.

which can be rewritten as

$$\left[\Delta - \left(\frac{3}{4}g_{23}^2 M - \frac{\delta}{2}\right)\right]^2 \simeq T' + \frac{3}{4}g_{H_2 VV}^2 \delta M + \left(\frac{3}{4}g_{23}^2 M - \frac{\delta}{2}\right)^2$$

(45)

with $T' \equiv \frac{T}{0.18}(100 \text{ GeV})^2$ using $\sqrt{2}G_F/16\pi^2\alpha_{\text{EM}} \simeq 1.337 \times 10^{-5}/\text{GeV}^2$. Note that the right-hand side of the above equation is positive definite unless $T < 0$, $\Delta = 0$ cannot satisfy the above relation, and the region of Δ with a radius smaller than $\sqrt{T'}$ around the point $\Delta = 3g_{23}^2 M/4 - \delta/2$ should not be allowed. For example, if $T \gtrsim 0.18$, the region of $|\Delta| \lesssim 100$ GeV should be excluded in the limit of $\delta = g_{23}^2 = 0$. In fact, we have checked that T is negative definite when $\Delta = 0$ using the full analytic expressions for the T parameter without resorting to the approximations, see Eqs. (31) and (32).[12]

As shown in our previous work [4], the quartic coupling Z_4 plays the crucial role to understand the upper limit on the mass scale of heavy Higgs bosons. We find that the expression for Z_4 in Eq. (11) can be recast as

$$Z_4 v^2 = 2(2\Delta + \delta)M + (\Delta + \delta)\delta$$
$$- \left[2g_{23}^2 M^2 + 2(g_{23}^2 \Delta + g_{H_3 VV}^2 \delta)M\right.$$
$$\left. + g_{23}^2\left(\frac{\Delta^2}{2} - 2M_{H_1}^2\right) + g_{H_3 VV}^2(\Delta + \delta)\delta\right], \quad (46)$$

in terms of Δ, δ, M, g_{23}^2, $g_{H_3 VV}^2$, and M_{H_1}. When $g_{23}^2 = 0$ and $\delta = 0$, using the above equation together with Eq. (42), we have

$$T \simeq 0.18\left(\frac{\Delta}{100 \text{ GeV}}\right)^2 \quad \text{or} \quad |\Delta| \simeq 100\sqrt{\frac{T}{0.18}}\text{GeV},$$
$$S \simeq 0.0053\left(\frac{\Delta}{100 \text{ GeV}}\right)\left(\frac{1 \text{ TeV}}{M}\right),$$
$$Z_4 \simeq 4\frac{\Delta M}{v^2} \simeq 6.6\left(\frac{\Delta}{100 \text{ GeV}}\right)\left(\frac{M}{1 \text{ TeV}}\right), \quad (47)$$

where we use $\sqrt{2}G_F/16\pi^2\alpha_{\text{EM}} \simeq 1.337 \times 10^{-5}/\text{GeV}^2$ and $v = 246.22$ GeV. Note that the UNIT $\oplus$ BFB constraint of $|Z_4| \lesssim 6.6$ leads to the upper limit of about 1 TeV on the heavy-Higgs mass scale M when $|\Delta| \simeq 100$ GeV. These are the main ingredients of our previous work [4].

In this work, we extend our analytic study on the mass spectrum of heavy Higgs bosons taking account of the effects of the mass splitting δ between the two neutral heavy Higgs bosons and the deviation from the alignment limit of $g_{23}^2 = 0$. Assuming the mass hierarchy $M \gg M_{H_1} \sim |\Delta| \gtrsim \delta$ given by Eq. (40) and keeping the leading terms in Eq. (46), one might approximate the expression for Z_4 as follow:

$$Z_4 v^2 \simeq (4\Delta + 2\delta)M - 2g_{23}^2 M^2. \quad (48)$$

It is interesting and illuminating to observe that each term of the above equation involves its own physics origin. The term containing Z_4 is constrained by the UNIT $\oplus$ BFB condition. The first term in the right-hand side involves the mass splittings among the heavy Higgs bosons and the high-precision CDF measurement of the W boson mass implies nonvanishing value for, especially, the mass splitting Δ between the charged and the second heaviest neutral Higgs bosons. The second term in the right-hand side is proportional to M^2 and it quickly increases when g_{23}^2 deviates from the alignment limit of $g_{23}^2 = 0$ or when the coupling $g_{H_1 VV}$ deviates from its SM value of 1.

Equation (48) can be rewritten for M as

$$g_{23}^2 M^2 - 2\hat{\Delta}M + 2\hat{\Delta}\hat{M}_0 \simeq 0, \quad (49)$$

by introducing

$$\hat{\Delta} \equiv \Delta + \frac{\delta}{2}, \qquad \hat{M}_0 \equiv \frac{Z_4 v^2}{4\Delta + 2\delta} = \frac{Z_4 v^2}{4\hat{\Delta}}. \quad (50)$$

When the discriminant $-2g_{23}^2\hat{\Delta}\hat{M}_0 + \hat{\Delta}^2 > 0$, Eq. (49) can be solved for M. By denoting the solution as M_{Z_4}, we obtain[13]:

$$\textbf{23C}\colon M_{Z_4} \simeq \frac{|\hat{\Delta}|}{g_{23}^2}\left[-1 + \left(1 - 2g_{23}^2\frac{\hat{M}_0}{\hat{\Delta}}\right)^{1/2}\right] \quad \text{when} \quad \hat{\Delta} < 0 \quad \text{and} \quad 2g_{23}^2\hat{M}_0 > -|\hat{\Delta}|,$$

$$\textbf{C23}\colon M_{Z_4} \simeq \frac{\hat{\Delta}}{g_{23}^2}\left[1 - \left(1 - 2g_{23}^2\frac{\hat{M}_0}{\hat{\Delta}}\right)^{1/2}\right] \quad \text{when} \quad \hat{\Delta} > 0 \quad \text{and} \quad 2g_{23}^2\hat{M}_0 < \hat{\Delta}. \quad (51)$$

---

[12]In fact, T is identically vanishing when $\Delta = \delta = 0$. We find that the same thing happens also when $\Delta = M_{H_2} - M_{H_1} = 0$.

[13]Note that $\hat{\Delta}$ has the same sign as Δ and $\hat{M}_0 > 0$ when $M \gtrsim 500$ GeV and $|\Delta| \gtrsim \delta$.
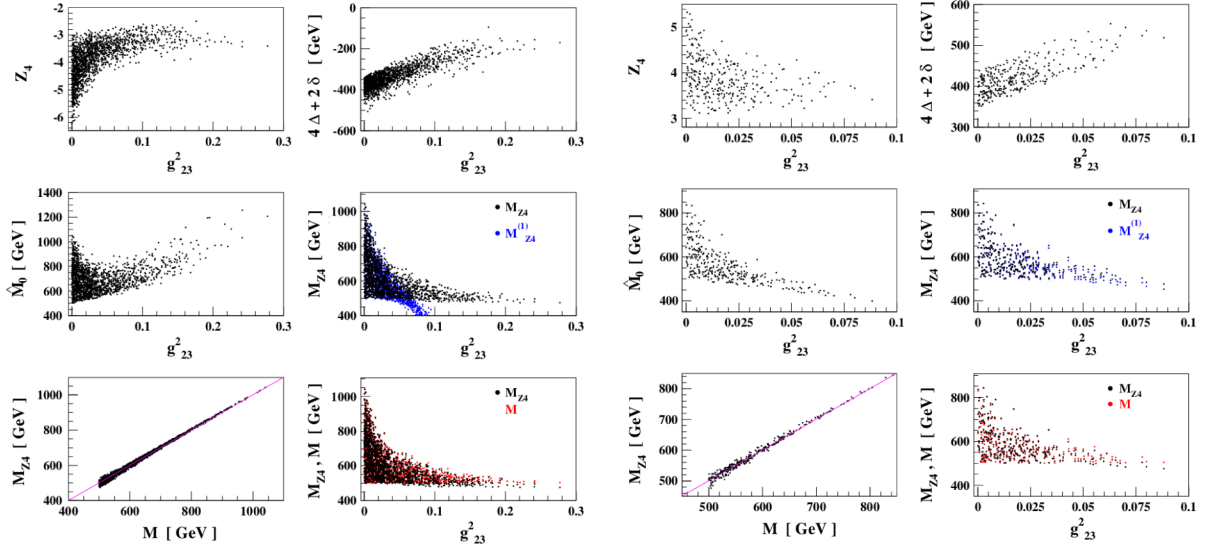
FIG. 6.   CDF: Behaviors of Z_4 (upper-left), $4\Delta + 2\delta$ (upper-right), $\hat{M}_0$ (middle-left), and M_{Z_4} and $M_{Z_4}^{(1)}$ (middle-right) according to the variation of g_{23}^2 and comparisons of M_{Z_4} and M (lower) for the 23C (left) and C23 (right) hierarchies with the magenta lines for $M_{Z_4} = M$. Note that M_{Z_4} and $M_{Z_4}^{(1)}$ are given by Eq. (51) and Eq. (53), respectively. The combined UNIT $\oplus$ BFB $\oplus$ ELW$_{95\%}$ constraints are imposed and $M > 500$ GeV is required.

When $g_{23}^2 |\hat{M}_0/\hat{\Delta}| \lesssim 1$, and one may expand M_{Z_4} as

$$M_{Z_4} \simeq \hat{M}_0 \left[1 + \frac{g_{23}^2}{2} \frac{\hat{M}_0}{\hat{\Delta}} + \frac{g_{23}^4}{2} \left(\frac{\hat{M}_0}{\hat{\Delta}} \right)^2 + \mathcal{O}\left(g_{23}^2 \frac{\hat{M}_0}{\hat{\Delta}} \right)^3 \right]$$

(52)

and, keeping the leading term in g_{23}^2, we define

$$M_{Z_4}^{(1)} \equiv \hat{M}_0 \left[1 + \frac{g_{23}^2}{2} \frac{\hat{M}_0}{\hat{\Delta}} \right].$$

(53)

Note that the quartic coupling Z_4 and the quantities $\hat{\Delta} = \Delta + \delta/2$ and $\hat{M}_0 = Z_4 v^2/4\hat{\Delta}$ possess their own *implicit* dependence on g_{23}^2 as will be shown shortly.

In the left panel of Fig. 6, we show the scatter plots for Z_4 versus g_{23}^2 (upper left), $4\Delta + 2\delta$ versus g_{23}^2 (upper right), $\hat{M}_0$ versus g_{23}^2 (middle left), and M_{Z_4} and $M_{Z_4}^{(1)}$ versus g_{23}^2 (middle right) for the 23C hierarchy with $\Delta < 0$. The combined UNIT $\oplus$ BFB $\oplus$ ELW$_{95\%}$ constraints have been imposed and $M > 500$ GeV is required. We observe that $|Z_4|$ takes its maximum value of about 6.3 at $g_{23}^2 = 0$ where $350 \lesssim |4\Delta + 2\delta|/\text{GeV} \lesssim 450$ which leads to $\hat{M}_0 = Z_4 v^2/(4\Delta + 2\delta) \lesssim 1050$ GeV in the alignment limit. As g_{23}^2 deviates from 0, the maximum value of $|Z_4|$ decreases quickly from ~ 6.3 to ~ 4 as g_{23}^2 reaches to 0.05 and, from there, it does not change much. On the other hand, the minimum value of $|4\Delta + 2\delta|$ almost uniformly decreases as g_{23}^2 increases. These combined features explain the behavior of $\hat{M}_0$ shown the middle-left frame.

In the middle-right frame, we show M_{Z_4} and $M_{Z_4}^{(1)}$ which are given by Eq. (51) and Eq. (53), respectively. We observe that, for the small values of $g_{23}^2 \lesssim 0.05$, M_{Z_4} is fairly well approximated by $M_{Z_4}^{(1)}$ which contains the proportionality factor $1 + g_{23}^2 \hat{M}_0/2\hat{\Delta}$ pulling down $\hat{M}_0$ as g_{23}^2 increases since $\hat{\Delta} < 0$ for the 23C hierarchy. In the lower frames, we compare M_{Z_4} obtained by solving Eq. (49) and the average mass scale $M = (M_{H^\pm} + M_{H_2})/2$. We find that $M_{Z_4} \simeq M$ with $|M_{Z_4} - M| \lesssim 30$ GeV and, therefore, conclude that M_{Z_4} excellently represents the heavy-Higgs mass scale M especially for the small values of g_{23}^2. This implies that we have fully figured out the physics origins relevant for the mass scale of heavy Higgs bosons by showing that it has been determined by combining the UNIT $\oplus$ BFB condition, the mass splittings among the heavy Higgs bosons, and deviation from the alignment limit.

In the right panel of Fig. 6, we show the same as in the left panel but for the C23 hierarchy with $\Delta > 0$. Similar observations could be made as in the left panel except that: (i) g_{23}^2 is constrained to be smaller than about 0.1 indicated by the condition $2g_{23}^2 \hat{M}_0 < \hat{\Delta}$, (ii) $Z_4 \lesssim 5.3$ leading to the smaller values of $\hat{M}_0 \lesssim 850$ GeV, (iii) now $\hat{M}_0$ is pushed up by the factor $1 + g_{23}^2 \hat{M}_0/2\hat{\Delta}$ since $\hat{\Delta} > 0$, and (iv) $M_{Z_4}^{(1)}$ provides the excellent approximation for M_{Z_4}. Otherwise, we confirm again that we have fully figured out the physics origins relevant for the mass scale of heavy Higgs bosons also in this case.

To conclude, for a given value of g_{23}^2, the upper limit on the average mass scale $M = (M_{H^\pm} + M_{H_2})/2$ is given by

the maximum value of M_{Z_4} which could be approximated by $M_{Z_4}^{(1)}$ when $g_{23}^2 \lesssim 0.05$:

$$M \lesssim \max(M_{Z_4}) \simeq \max[M_{Z_4}^{(1)}], \qquad (54)$$

and then

$$M_{H_2} = M + \Delta/2 \lesssim \max[M_{Z_4}^{(1)}] + \Delta/2,$$
$$M_{H^\pm} = M - \Delta/2 \lesssim \max[M_{Z_4}^{(1)}] - \Delta/2, \qquad (55)$$

for the both 23C ($\Delta < 0$) and C23 ($\Delta > 0$) hierarchies. In this section, taking the CDF values given in Eq. (28), we find

$$\max[M_{Z_4}^{(1)}] = \max(\hat{M}_0) \simeq \begin{cases} 1050 \text{ GeV} & \text{for} \quad \mathbf{23C}(\Delta < 0) \\ 850 \text{ GeV} & \text{for} \quad \mathbf{C23}(\Delta > 0) \end{cases}, \qquad (56)$$

in the alignment limit which precisely reproduces the highest masses of the heavy neutral and charged Higgs bosons shown in Fig. 4 together with $|\Delta|_{M=\max(M)} \simeq 100$ GeV, see Eq. (34). Note that the 23C hierarchy leads to the heavier spectrum.

V. DISCUSSION

The specific values for the S and T parameters given in Eq. (28) are subject to changes depending on the details of

the available ELW precision data and how to collect and fit them. In this section, taking PDG and CDF as the two extreme limits, we discuss how the upper limit on the heavy-Higgs mass scale M changes by varying the values for the S and T parameters between PDG and CDF. More precisely, we vary the central values of the S and T parameters as

$$\hat{T}_0 = 0.22 t_{EW} + 0.05, \qquad \hat{S}_0 = 0.15 t_{EW} \qquad (57)$$

with the parameter t_{EW} scanned between 0 and 1. For σ_S, σ_T, and ρ_{ST}, we take the CDF values as in Eq. (28). Now, the heavy Higgs masses squared are scanned up to $(3 \text{ TeV})^2$ since we expect the smaller mass splitting $|\Delta|$ with $\hat{T}_0 < 0.27$ which might lead to the upper limit on M larger than 1 TeV. Further we take $\gamma = \eta = 0$ because M_{Z_4} takes its maximum value in the alignment limit, see the middle frames in Fig. 6. Otherwise, the parameters are scanned as described at the end of Sec. II.

The left panel of Fig. 7 are for the scatter plots for $\hat{T}_0$ versus t_{EW} (upper left) and $\hat{T}_0$ versus $\hat{S}_0$ (upper right) according to Eq. (57). The lower-left frame is for T versus S obtained by imposing the combined UNIT $\oplus$ BFB $\oplus$ ELW$_{95\%}$ constraints. Comparing with Fig. 2, we observe that the scattered dots are more centered around $S = 0$ with $T > 0$. The lower-right frame is for Δ versus δ with the magenta lines for $|\Delta| = \delta$. The colored dots are for $t_{EW} > 0.05$ (black + red + blue), $t_{EW} > 0.5$ (red + blue),

FIG. 7. Between PDG and CDF: $\hat{T}_0 = 0.22 t_{EW} + 0.05$ and $\hat{S}_0 = 0.15 t_{EW}$ with $0 \le t_{EW} \le 1$ taking the CDF values for $\sigma_S = 0.08$, $\sigma_T = 0.06$, and $\rho_{ST} = 0.93$. The alignment limit of $\gamma = \eta = 0$ has been taken, the heavy Higgs masses squared are scanned up to $(3 \text{ TeV})^2$, and the other parameters are scanned as described at the end of Sec. II. The combined UNIT $\oplus$ BFB $\oplus$ ELW$_{95\%}$ constraints have been imposed. (Left) The magenta lines in the lower-right frame are for $|\Delta| = \delta$ and the colored dots are for $t_{EW} > 0.05$ (black + red + bl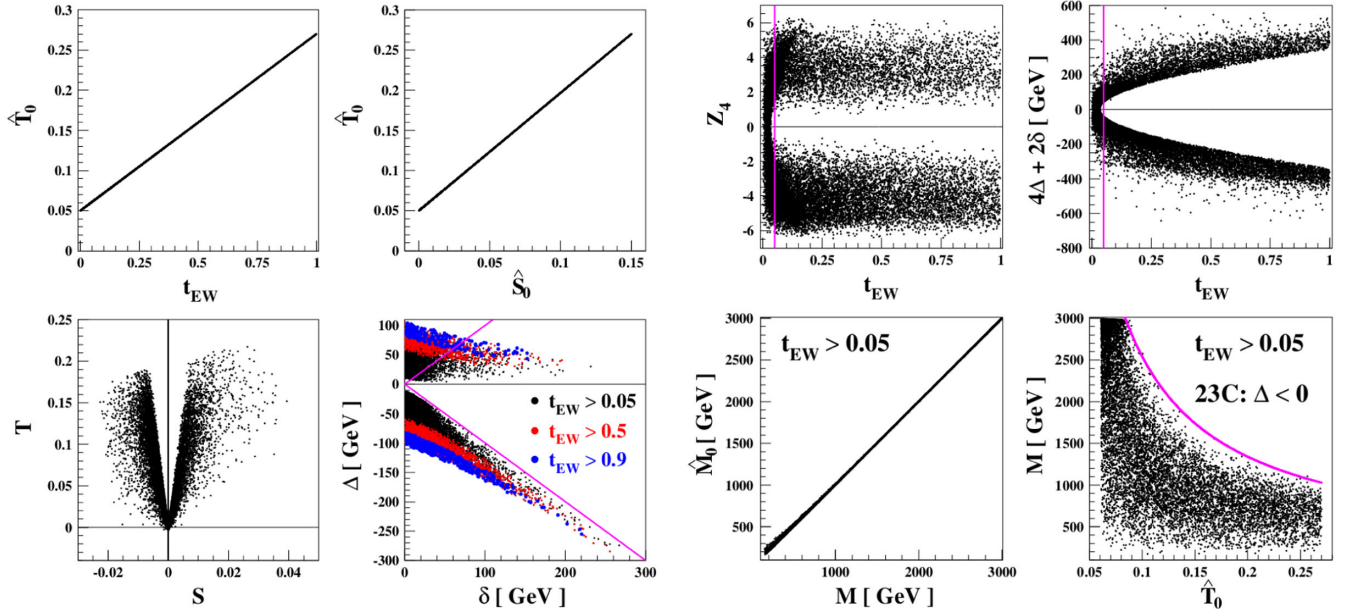ue), $t_{EW} > 0.5$ (red + blue), and $t_{EW} > 0.9$ (blue). (Right) The vertical magenta lines in the upper frames denotes the position $t_{EW} = 0.05$ and the magenta curve in the lower-right frame represents the case $M = 240/\hat{T}_0 + 140$ GeV.

and $t_{EW} > 0.9$ (blue). First of all, we note that the nonvanishing mass splitting $|\Delta|$ is required if $\hat{T}_0$ deviates from 0 by more than $1\sigma_T = 0.06$ or, equivalently, $t_{EW} > 0.05$. And, as expected, the larger mass splitting $|\Delta|$ is needed to accommodate the larger value of $\hat{T}_0$. We note that $|\Delta| \simeq 100$ GeV when $\delta = 0$ in the CDF limit of $t_{EW} = 1$. When $\Delta < 0$, $|\Delta| > \delta$ resulting in the 23C hierarchy independently of t_{EW} and M.

In the upper frames of the right panel of Fig. 7, we show the scatter plots for Z_4 versus t_{EW} (upper left) and $4\Delta + 2\delta$ versus t_{EW} (upper right). From $t_{EW} \simeq 0.05$ denoted by the vertical magenta lines, the region around $|Z_4| = 0$ starts to be excluded and $|4\Delta + 2\delta|$ begins to deviate from 0 implying that the upper limit on M emerges. Note that the allowed regions of the quartic coupling Z_4 are almost independent of t_{EW} once it is larger than 0.05. In the lower-left frame, we show the scatter plot for $\hat{M}_0$ versus M for $t_{EW} > 0.05$. We observe that the scattered points are distributed along the $\hat{M}_0 = M$ line with $|\hat{M}_0 - M| < 20$ GeV for $M > 1$ TeV[14] implying that the mass scale of heavy Higgs bosons originates from the UNIT $\oplus$ BFB constraint on the quartic coupling Z_4 and the mass splittings among the heavy Higgs bosons. In the lower-right frame, taking $t_{EW} > 0.05$, we show the scatter plot for M versus $\hat{T}_0$ for the 23C hierarchy ($\Delta < 0$) which predicts the heavier mass spectrum compared to the C23 hierarchy with $\Delta > 0$. We observe that the heavy Higgs bosons should exist below 2.5(1.3) TeV if $\hat{T}_0 > 0.1(0.2)$. Incidentally, we find that

$$M \lesssim \left(\frac{240}{\hat{T}_0} + 140 \right) \text{ GeV}, \tag{58}$$

as denoted by the magenta curve in the lower-right frame. This empirical relation could be used to derive the conservative $\hat{T}_0$-dependent upper limit on M more conveniently.

Last but not least, for the searches of heavy Higgs bosons at future colliders such as the high luminosity option of the LHC (HL-LHC) and a 100 TeV hadron collider, we propose some benchmarking scenarios in which the masses of the heavy Higgs bosons saturate their upper limits for a given value of $\hat{T}_0$, see Table I. In the proposed saturating scenarios, the heavy neutral Higgs bosons are almost degenerate. The heavier spectrum is predicted for the larger value of $\hat{T}_0$ and we note that the heavy Higgs bosons are lighter than 3 TeV for $\hat{T}_0 > 0.09$. When $\hat{T}_0 \gtrsim 0.21$, the heavy Higgs bosons weighing around 1 TeV and the on-shell W boson coming from the decay of the charged Higgs boson (23C) or the heavy neutral Higgs bosons (C23) might be signatures of the scenarios with

---

[14]In the alignment of $g_{23}^2 = 0$, $M_{Z_4} = \hat{M}_0 = Z_4 v^2/(4\Delta + 2\delta)$, see Eq. (49).

TABLE I. Benchmarking scenarios in which the masses of the heavy Higgs bosons saturate their upper limits for a given value of $\hat{T}_0$. We take the four values of $\hat{T}_0$ from the CDF value of 0.27 to 0.09 in decrement of $\sigma_T = 0.06$ with $\hat{S}_0 = 0.15(\hat{T}_0 - 0.05)/0.22$, see Eq. (57).

	23C		C23	
	$M_{H_2} \simeq M_{H_3}$	$M_{H^\pm}$	$M_{H_2} \simeq M_{H_3}$	$M_{H^\pm}$
$(\hat{T}_0, \hat{S}_0)$	(GeV)	(GeV)	(GeV)	(GeV)
(0.27, 0.15)	1000	1100	900	800
(0.21, 0.11)	1100	1180	1090	1010
(0.15, 0.07)	1640	1700	1540	1480
(0.09, 0.03)	2730	2760	2630	2600

$|g_{H_{2,3}H^\pm W^\mp}| \simeq 1$ [54]. For $\hat{T}_0 \lesssim 0.15$, the heavy Higgs bosons are located above 1.5 TeV and the mass difference between the charged and neutral Higgs bosons is smaller than 60 GeV. They might be out of the reach of the HL-LHC but well within the reach of a 100 TeV hadron collider [55,56].

VI. CONCLUSIONS

We analyze the implication of the large positive deviation of the S and T parameters from the SM values of zero indicated by the high-precision CDF measurement of the W boson mass on the mass spectrum of heavy Higgs bosons considering the most general CP-violating 2HDM potential. We show that the mass splitting between the charged Higgs boson and the second heaviest neutral one is necessary to accommodate the sizable positive value of the T parameter especially. Combining with the theoretical constraints on the quartic couplings from the perturbative unitarity and for the Higgs potential to be bounded from below, we provide the comprehensive analysis why the masses of the heavy Higgs bosons should be bounded from above.

We further suggest the following points as the main results of this work:

(1) We clearly demonstrate that there exist only two rephasing-invariant CPV phases of $\theta_1 = \text{Arg}[Z_6(Z_5^*)^{1/2}]$ and $\theta_2 = \text{Arg}[Z_7(Z_5^*)^{1/2}]$ in the CPV 2HDM Higgs potential pivoting around the complex quartic coupling Z_5. Note that the second angle θ_2 has nothing to do with the masses of Higgs bosons and the mixing of the neutral ones.

(2) By imposing the combined UNIT $\oplus$ BFB $\oplus$ ELW$_{95\%}$ constraints and taking the CDF values for the S and T parameters, we find

$$0.1 \lesssim Z_1 \lesssim 2.0, \quad 0 \lesssim Z_2 \lesssim 2.1, \quad -2.6 \lesssim Z_3 \lesssim 8.0,$$

$$-6.3 \lesssim Z_4 \lesssim -0.8 \cup 1.1 \lesssim Z_4 \lesssim 5.4,$$

$$|Z_5| \lesssim 1.7, \quad |Z_6| \lesssim 2.4, \quad |Z_7| \lesssim 2.7.$$

Note that the ranges of the quartic couplings appearing in the Higgs potential are largely independent of the ELW constraint except that the region with $|Z_4| \lesssim 1$ is excluded by the large value of the T parameter.

(3) Concentrating on the heavy mass region $M = (M_{H_2} + M_{H^\pm})/2 \gtrsim 500$ GeV in which we find a mass hierarchy of $M \gg M_{H_1} \sim |\Delta| \gtrsim \delta$ with $\Delta = M_{H_2} - M_{H^\pm}$ and $\delta = M_{H_3} - M_{H_2}$, we figure out that there could be the following two types of mass spectrum

$$\mathbf{23C}: \; M_{H_2} < M_{H_3} < M_{H^\pm} \quad \text{when } \Delta < 0 \quad \text{and} \quad \delta < |\Delta|;$$

$$\mathbf{C23}: \; M_{H^\pm} < M_{H_2} < M_{H_3} \quad \text{when } \Delta > 0 \text{ independently of } \delta.$$

When $\Delta < 0$, note that one can achieve the hierarchy $M_{H_3} < M_{H^\pm}$ if $M \gtrsim 500$ GeV or in the alignment limit.

(4) The upper limit on the masses of heavy Higgs bosons becomes stronger when the effects of deviation from the alignment limit are taken into account. In the CDF case, we show that the upper limit on M changes from about 1 TeV to about 700 GeV as g_{23}^2 deviates from 0 to 0.05 for the 23C hierarchy.

(5) We have fully figured out the physics origins relevant for the mass scale of heavy Higgs bosons by showing that the heavy-Higgs mass scale M could be excellently represented by M_{Z_4} obtained by solving Eq. (49) which incorporates. (i) the UNIT $\oplus$ BFB condition, (ii) the mass splittings among the heavy Higgs bosons, and (iii) the deviation from the alignment limit.

(6) When $M \lesssim 3$ TeV, we provide the following useful and convenient empirical $\hat{T}_0$-dependent upper limit:

$$M \lesssim \left(\frac{240}{\hat{T}_0} + 140 \right) \text{ GeV},$$

obtained by varying the central values of the S and T parameters between PDG and CDF given by Eq. (28).

(7) We propose some $\hat{T}_0$-dependent benchmarking scenarios in which the masses of the heavy Higgs bosons saturate their upper limits for a given value of $\hat{T}_0$, see Table I. For the CDF values given in Eq. (28), we propose the following two sat-CDF scenarios:

$$\mathbf{23C}_{\texttt{sat-CDF}}: \; M_{H_2} \simeq M_{H_3} \simeq 1000 \text{ GeV}, \qquad M_{H^\pm} \simeq 1100 \text{ GeV};$$

$$\mathbf{C23}_{\texttt{sat-CDF}}: \; M_{H^\pm} \simeq 800 \text{ GeV}, \qquad M_{H_2} \simeq M_{H_3} \simeq 900 \text{ GeV}.$$

[1] T. Aaltonen *et al.* (CDF Collaboration), High-precision measurement of the *W* boson mass with the CDF II detector, Science **376**, 170 (2022).

[2] P. A. Zyla *et al.* (Particle Data Group), Review of particle physics, Prog. Theor. Exp. Phys. **2020**, 083C01 (2020).

[3] C. T. Lu, L. Wu, Y. Wu, and B. Zhu, Electroweak precision fit and new physics in light of the *W* boson mass, Phys. Rev. D **106**, 035034 (2022).

[4] Y. Heo, D. W. Jung, and J. S. Lee, Impact of the CDF W-mass anomaly on two Higgs doublet model, Phys. Lett. B **833** (2022), 137274.

[5] S. Lee, K. Cheung, J. Kim, C. T. Lu, and J. Song, Status of the two-Higgs-doublet model in light of the CDF m_W measurement, Phys. Rev. D **106**, 075013 (2022).

[6] Y. Z. Fan, T. P. Tang, Y. L. S. Tsai, and L. Wu, Inert Higgs Dark Matter for CDF II W-Boson Mass and Detection Prospects, Phys. Rev. Lett. **129**, 091802 (2022).

[7] H. Song, W. Su, and M. Zhang, Electroweak phase transition in 2HDM under Higgs, Z-pole, and W precision measurements, J. High Energy Phys. 10 (2022) 048.

[8] H. Bahl, J. Braathen, and G. Weiglein, New physics effects on the W-boson mass from a doublet extension of the SM Higgs sector, Phys. Lett. B **833**, 137295 (2022).

[9] K. S. Babu, S. Jana, and V. P. K., Correlating W-Boson Mass Shift with Muon $g - 2$ in the 2HDM, Phys. Rev. Lett. **129**, 121803 (2022).

[10] Y. H. Ahn, S. K. Kang, and R. Ramos, Implications of the new CDF II W-boson mass on two-Higgs-doublet models, Phys. Rev. D **106**, 055038 (2022).

[11] X. F. Han, F. Wang, L. Wang, J. M. Yang, and Y. Zhang, Joint explanation of W-mass and muon g–2 in the 2HDM*, Chin. Phys. C **46**, 103105 (2022).

[12] G. Arcadi and A. Djouadi, The 2HD + a model for a combined explanation of the possible excesses in the CDF $\mathbf{M_W}$ measurement and $(\mathbf{g - 2})_\mu$ with dark matter, Phys. Rev. D **106**, 095008 (2022).

[13] K. Ghorbani and P. Ghorbani, W-boson mass anomaly from scale invariant 2HDM, Nucl. Phys. **B984**, 115980 (2022).

[14] R. Benbrik, M. Boukidi, and B. Manaut, W-mass and 96 GeV excess in type-III 2HDM, arXiv:2204.11755.

[15] H. Abouabid, A. Arhrib, R. Benbrik, M. Krab, and M. Ouchemhou, Is the new CDF M_W measurement consistent with the two higgs doublet model?, Nucl. Phys. **B989**, 116143 (2023).

[16] F. J. Botella, F. Cornet-Gomez, C. Miró, and M. Nebot, Muon and electron $g - 2$ anomalies in a flavor conserving 2HDM with an oblique view on the CDF M_W value, Eur. Phys. J. C **82**, 915 (2022).

[17] J. Kim, Compatibility of muon g-2, W mass anomaly in type-X 2HDM, Phys. Lett. B **832**, 137220 (2022).

[18] J. Kim, S. Lee, P. Sanyal, and J. Song, CDF W-boson mass and muon g-2 in a type-X two-Higgs-doublet model with a Higgs-phobic light pseudoscalar, Phys. Rev. D **106**, 035002 (2022).

[19] T. Appelquist, J. Ingoldby, and M. Piai, Composite two-Higgs doublet model from dilaton effective field theory, Nucl. Phys. **B983**, 115930 (2022).

[20] O. Atkinson, M. Black, C. Englert, A. Lenz, and A. Rusov, MUonE, muon $g - 2$ and electroweak precision constraints within 2HDMs, Phys. Rev. D **106**, 115031 (2022).

[21] S. Hessenberger and W. Hollik, Two-loop improved predictions for M_W and $\sin^2 \theta_{\text{eff}}$ in two-Higgs-doublet models, Eur. Phys. J. C **82**, 970 (2022).

[22] J. Kim, S. Lee, J. Song, and P. Sanyal, Fermiophobic light Higgs boson in the type-I two-Higgs-doublet model, Phys. Lett. B **834**, 137406 (2022).

[23] F. Arco, S. Heinemeyer, and M. J. Herrero, Sensitivity and constraints to the 2HDM soft-breaking Z_2 parameter m_{12}, Phys. Lett. B **835**, 137548 (2022).

[24] S. K. Kang, J. Kim, S. Lee, and J. Song, Disentangling the high and low cutoff scales via the trilinear Higgs couplings

[25] G. Kumar, Interplay of the charged Higgs effects in $R_{D^{(*)}}$, $b \to s\ell^+\ell^-$ and W-mass, Phys. Rev. D **107**, 075016 (2023).

[26] J. F. Donoghue and L. F. Li, Properties of charged Higgs bosons, Phys. Rev. D **19**, 945 (1979).

[27] H. Georgi and D. V. Nanopoulos, Suppression of flavor changing effects from neutral spinless meson exchange in gauge theories, Phys. Lett. **82B**, 95 (1979).

[28] J. S. Lee and J. Park, Yukawa alignment revisited in the Higgs basis, Phys. Rev. D **106**, 015023 (2022).

[29] H. E. Haber and D. O'Neil, Basis-independent methods for the two-Higgs-doublet model. II. The significance of tan β, Phys. Rev. D **74**, 015018 (2006); **74**, 059905(E) (2006).

[30] H. E. Haber and D. O'Neil, Basis-independent methods for the two-Higgs-doublet model III: The CP-conserving limit, custodial symmetry, and the oblique parameters S, T, U, Phys. Rev. D **83**, 055017 (2011).

[31] I. F. Ginzburg and I. P. Ivanov, Tree-level unitarity constraints in the most general 2HDM, Phys. Rev. D **72**, 115010 (2005).

[32] S. Kanemura and K. Yagyu, Unitarity bound in the most general two Higgs doublet model, Phys. Lett. B **751**, 289 (2015).

[33] D. Jurčiukonis and L. Lavoura, The three- and four-Higgs couplings in the general two-Higgs-doublet model, J. High Energy Phys. 12 (2018) 004.

[34] M. Maniatis, A. von Manteuffel, O. Nachtmann, and F. Nagel, Stability and symmetry breaking in the general two-Higgs-doublet model, Eur. Phys. J. C **48**, 805 (2006).

[35] I. P. Ivanov, Minkowski space structure of the Higgs potential in 2HDM, Phys. Rev. D **75**, 035001 (2007); **76**, 039902(E) (2007).

[36] I. P. Ivanov, Minkowski space structure of the Higgs potential in 2HDM. II. Minima, symmetries, and topology, Phys. Rev. D **77**, 015017 (2008).

[37] I. P. Ivanov and J. P. Silva, Tree-level metastability bounds for the most general two Higgs doublet model, Phys. Rev. D **92**, 055017 (2015).

[38] H. Bahl, M. Carena, N. M. Coyle, A. Ireland, and C. E. M. Wagner, New tools for dissecting the general 2HDM, J. High Energy Phys. 03 (2023) 165.

[39] G. C. Branco, P. M. Ferreira, L. Lavoura, M. N. Rebelo, M. Sher, and J. P. Silva, Theory and phenomenology of two-Higgs-doublet models, Phys. Rep. **516**, 1 (2012).

[40] M. E. Peskin and T. Takeuchi, A New Constraint on a Strongly Interacting Higgs Sector, Phys. Rev. Lett. **65**, 964 (1990).

[41] M. E. Peskin and T. Takeuchi, Estimation of oblique electroweak corrections, Phys. Rev. D **46**, 381 (1992).

[42] J. S. Lee and A. Pilaftsis, Radiative corrections to scalar masses and mixing in a scale invariant two Higgs doublet model, Phys. Rev. D **86**, 035004 (2012).

[43] D. Toussaint, Renormalization effects from superheavy Higgs particles, Phys. Rev. D **18**, 1626 (1978).

[44] W. Grimus, L. Lavoura, O. M. Ogreid, and P. Osland, A precision constraint on multi-Higgs-doublet models, J. Phys. G **35**, 075001 (2008).

[45] W. Grimus, L. Lavoura, O. M. Ogreid, and P. Osland, The oblique parameters in multi-Higgs-doublet models, Nucl. Phys. **B801**, 81 (2008).

[46] M. Misiak, A. Rehman, and M. Steinhauser, Towards $\bar{B} \to X_s\gamma$ at the NNLO in QCD without interpolation in m_c, J. High Energy Phys. 06 (2020) 175.

[47] A. Pich and P. Tuzon, Yukawa alignment in the two-Higgs-doublet model, Phys. Rev. D **80**, 091702 (2009).

[48] S. L. Glashow and S. Weinberg, Natural conservation laws for neutral currents, Phys. Rev. D **15**, 1958 (1977).

[49] J. M. Connell, P. Ferreira, and H. E. Haber, Accommodating hints of new heavy scalars in the framework of the flavor-aligned two-Higgs-doublet model, arXiv:2302.13697.

[50] K. Cheung, J. S. Lee, and P. Y. Tseng, New emerging results in Higgs precision analysis updates 2018 after establishment of third-generation Yukawa couplings, J. High Energy Phys. 09 (2019) 098.

[51] ATLAS Collaboration, A combination of measurements of Higgs boson production and decay using up to 139 fb^{-1} of proton–proton collision data at $\sqrt{s} = 13$ TeV collected with the ATLAS experiment, Report No. ATLAS-CONF-2020-027.

[52] CMS Collaboration, Combined Higgs boson production and decay measurements with up to 137 fb^{-1} of proton-proton collision data at $\sqrt{s} = 13$ TeV, Report No. CMS-PAS-HIG-19-005.

[53] G. Aad *et al.* (ATLAS Collaboration), Combined measurements of Higgs boson production and decay using up to 80 fb^{-1} of proton-proton collision data at $\sqrt{s} = 13$ TeV collected with the ATLAS experiment, Phys. Rev. D **101**, 012002 (2020).

[54] See, for example, S. Y. Choi, J. S. Lee, and J. Park, Decays of Higgs bosons in the standard model and beyond, Prog. Part. Nucl. Phys. **120**, 103880 (2021).

[55] J. Hajer, Y. Y. Li, T. Liu, and J. F. H. Shiu, Heavy Higgs bosons at 14 TeV and 100 TeV, J. High Energy Phys. 11 (2015) 124.

[56] N. Arkani-Hamed, T. Han, M. Mangano, and L. T. Wang, Physics opportunities of a 100 TeV proton–proton collider, Phys. Rep. **652**, 1 (2016).